Submitted to Phys. Rev.

UCRL-20856

c.2

# EXPERIMENTAL RESULTS ON THE REACTIONS $\pi^- p \rightarrow \pi\pi N$ IN THE C.M. ENERGY RANGE 1400 - 2000 MeV*

A. D. Brody, ** R. J. Cashmore, A. Kernan, *** D. W. G. S. Leith,
B. G. Levi, A. Minten, ** and B. C. Shen***

Stanford Linear Accelerator Center
Stanford University, Stanford, California 94305

J. P. Berge, ** B. Deler, D.J. Herndon, R. Longacre,
L. R. Miller, L. R. Price, A. H. Rosenfeld, P. Söding

Lawrence Radiation Laboratory
University of California, Berkeley, California 94720

TWO-WEEK LOAN COPY

This is a Library Circulating Copy
which may be borrowed for two weeks.
For a personal retention copy, call
Tech. Info. Division, Ext. 5545

UCRL-20856
c.2

## DISCLAIMER

This document was prepared as an account of work sponsored by the United States Government. While this document is believed to contain correct information, neither the United States Government nor any agency thereof, nor the Regents of the University of California, nor any of their employees, makes any warranty, express or implied, or assumes any legal responsibility for the accuracy, completeness, or usefulness of any information, apparatus, product, or process disclosed, or represents that its use would not infringe privately owned rights. Reference herein to any specific commercial product, process, or service by its trade name, trademark, manufacturer, or otherwise, does not necessarily constitute or imply its endorsement, recommendation, or favoring by the United States Government or any agency thereof, or the Regents of the University of California. The views and opinions of authors expressed herein do not necessarily state or reflect those of the United States Government or any agency thereof or the Regents of the University of California.

SLAC-PUB-911
UCRL-20856
June 1971
(TH) and (EXP)

c.1 c.2

# EXPERIMENTAL RESULTS ON THE REACTIONS $\pi^- p \rightarrow \pi\pi N$ IN THE C.M. ENERGY RANGE 1400 - 2000 MeV*

A. D. Brody,** R. J. Cashmore, A. Kernan,*** D.W.G.S. Leith, B. G. Levi, A. Minten,** and B. C. Shen***

Stanford Linear Accelerator Center
Stanford University, Stanford, California 94305

J. P. Berge,** B. Deler,† D. J. Herndon, R. Longacre, L. R. Miller, L. R. Price,†† A. H. Rosenfeld, P. Söding†††

Lawrence Radiation Laboratory
University of California, Berkeley, California 94720

RECEIVED
LAWRENCE
RADIATION LAB.
AUG 9 1971
LIBRARY
DOCUMENTS SEC.

## ABSTRACT

Cross sections and representative distributions are given for the reactions $\pi^- p \rightarrow \pi^+\pi^- n$, $\pi^- p \rightarrow \pi^- p\pi^0$ based on 85,000 inelastic events in the c.m. energy region 1400 - 2000 MeV. The angular distributions of beam, defined with respect to the final state particles are given in terms of their moments as a function of Dalitz plot position and c.m. energy.

(Submitted to Phys. Rev.)

*Work supported by the U. S. Atomic Energy Commission.

**Present address is CERN, Geneva, Switzerland.

***Present address is University of California, Riverside, California.

†Present address is Dept. de Physique des Particules Elementaires, CEN, Saclay, France.

††Present address is University of California, Irvine, California.

†††Present address is DESY, Hamburg, Germany.

REFERENCE
For Reference
Not to be taken from this room

## I. INTRODUCTION

Although the elastic and charge exchange channels of pion nucleon scattering experiments have been studied extensively,[1-8] the data on inelastic channels remains incomplete.[9] These channels are becoming more important since the phase shift analyses, which have been successful in revealing the major features of the $\pi N$ system, are in considerable disagreement over the detailed features of partial waves of low elasticity. For these reasons we have made systematic measurements of inelastic channels in the energy region 1400 - 2000 MeV.

The origin of these data are exposures of the 72" HBC at LRL and the 30" HBC at ANL to $\pi^-$ beams in the momentum range 550 MeV/c to 1600 MeV/c. This paper is concerned with the study of inelastic 2-prong events observed in this film, i.e.,

$$\pi^- p \longrightarrow \pi^+ \pi^- n \ . \ . \ . \quad \sim 51,000 \text{ events} \tag{1}$$

$$\pi^- p \longrightarrow \pi^- \pi^0 p \ . \ . \ . \quad \sim 34,000 \text{ events} \tag{2}$$

The other major contribution to the 2-prong topology comes from elastic scattering

$$\pi^- p \longrightarrow \pi^- p \quad . \ . \ . \quad \sim 80,000 \text{ events} \tag{3}$$

and this has been discussed previously.[10]

Within three c.m. energy regions, 1400 - 1600 MeV, 1600 - 1800 MeV, 1800 - 2000 MeV, our data correspond to approximate $\mu$b equivalents of 0.5 events/$\mu$b, 2.0 events/$\mu$b, 2.5 events $\mu$b, respectively.

In Section II we describe the identification of events from reactions (1) and (2) and other details of the data analysis. In Section III we give cross sections for these two channels and in Section IV we describe the general characteristics of the reactions and give the results of moments analysis of reactions (1) and (2) throughout our entire c.m. energy region. Section V contains the results of an analysis of the $\pi^+\pi^-n$ final state leading to a presentation of the $\Delta\pi$ and $\rho N$ partial cross sections.

The results of an analysis of the $\Delta^- \pi^+$ final state over a limited energy range are also summarized. Section VI contains only a short discussion of the results. The main purpose of this paper is a presentation of the experimental results. A detailed discussion of the partial wave analyses of the inelastic data now in progress will appear at a later date.

## II. DATA ANALYSIS

Details of the beams, experimental procedures, scanning and measuring, and data reduction have been described previously.[10] The film was scanned for all two prong events which were then subsequently measured on an LRL Spiral Reader. In this section we are only concerned with the identification of reactions (1) and (2).

An attempt is made to fit all two prong events with the hypotheses corresponding to reactions (1) - (3). Because the elastic scattering (3) is more highly constrained than the remaining one-constraint hypotheses, all events that satisfy this hypothesis with a chisquare for the kinematic fit, $\chi^2_K$, less than 25 were accepted as elastic scatters.

If an event satisfied either (1) or (2) only, with a value of $\chi^2_K$ less than a prescribed value $\left(\chi^2_K = 7 \text{ for the Argonne film and } \chi^2_K = 8 \text{ for the Berkeley film}\right)$ then that hypothesis was unambiguously selected. However, if an event satisfied both of these hypotheses, we adopt certain criteria to select the "best" fit. (In the Argonne film ~15% of inelastic events were ambiguous between the two interpretations (1) and (2) after just kinematical fitting. The corresponding number for the Berkeley film was ~18%). We considered not only the $\chi^2_K$ for the kinematic fit but also the $\chi^2_{ion}$ for the fit of the calculated ionization to that determined experimentally from pulse height measurements of the Spiral Reader. At the relatively low energies involved in the present experiment, the difference in ionization between a proton and a pion track can often be decisive. For the 72" Alvarez HBC film we used the

following selection criteria;

a) we chose that hypothesis which gave the lower value of the $\chi^2_{ion}$, provided the difference was larger than 3,

b) if the difference in $\chi^2_{ion}$ for the two fits was less than 3, we chose that hypothesis which gave the lower value of $\chi^2_K$, providing this difference was larger than 1.5,

c) if the difference in $\chi^2_K$ was also less than 1.5, we selected that hypothesis which gave the lower value of $\chi^2_{ion}$.

For the 30" MURA HBC film, we employed a simpler selection criterion. We formed a linear combination of $\chi^2_K$ and $\chi^2_{ion}$, which is called the combined chi-square, $\chi^2_{comb}$.[11] We assigned an ambiguous event to either reaction (1) or (2) depending on which fit gave the lower value of $\chi^2_{comb}$. To compare the results of the two selection procedures, we made the selection in both manners for a sample of events. The resulting identifications were essentially identical.

In Figs. 1 and 2 we present the pull quantities for the beam track, shown separately for the four experimental runs that comprise the experiment and the two reactions (1) and (2). In Figs. 3 and 4 we plot the chisquare values $\chi^2_K$, $\chi^2_{ion}$, and $\chi^2_{comb}$, while in Fig. 5 we show the missing mass squared of the missing particle in events assigned to reactions (1) and (2).

In order to study whether the ambiguities have been correctly resolved, we examine several quantities corresponding to the "wrong" hypothesis in the sample of ambiguous events. Figures 6 and 7 display the missing mass squared for both the "right" and "wrong" interpretations. The distributions for the "wrong" choice appear far too broad, especially in comparison with the corresponding plot for the "right" choice. The shaded histograms correspond to the samples of these events with $\chi^2_{ion}$ less than 12 for the "wrong" hypothesis. The distributions are not improved by this cut and thus none of these events are examples of the reaction corresponding to the

"wrong" choice. In Figs. 8 and 9 we show the $\chi^2_{ion}$ and $\chi^2_{comb}$ distributions corresponding to the "wrong" choice. They do not display the correct characteristics of two- and three-constraint fits. From these observations we have concluded that the selection criteria we have adopted are reasonable and introduce negligible contamination in the total sample of events.

After the events were measured, processed and separated according to the reaction type, we obtained a total of ~51,000 events in the final states $\pi^+\pi^-n$ and ~34,000 events in the final state $\pi^-\pi^0p$. The statistics, broken down by energy regions, are given in Table I. The energy is the central value determined from the corresponding sample of elastic scatters. We chose to use these values because of the higher statistics and smaller errors in this final state together with the fact that we used the elastic data for normalization in obtaining the cross sections.[10]

## III. CROSS SECTIONS

In determining the total elastic cross section we used a procedure of normalizing our data in a limited range of the angular distribution to counter measurements in the same region, after the necessary corrections had been made.[10] This then gives the cross section per event for the various energy regions of our film, both for the elastic and inelastic reactions. This procedure would be unsatisfactory if elastic events are fitted and accepted more efficiently than inelastic events. No evidence of this exists, the proportions of elastic and inelastic events being the same in both the first measurements of the data and the subsequent measurements of those events which initially failed.

In the case of the inelastic data we again investigated the distribution of events about the beam direction. We define a normal to the plane of the two outgoing tracks and look at the azimuthal distribution of this normal using a coordinate system in

which the camera axis is defined to be the x-axis and the beam direction the z-axis. A small loss of events is observed when the normal is perpendicular to the camera axis. The corrections for this effect are given in Table II and Fig. 10.

After making these corrections the cross sections for the two inelastic reactions are given in Table III, together with the total elastic cross section at the same energy.[10] Figures 11 and 12 display these inelastic cross sections while in Fig. 13 we compare the total cross section of A. A. Carter et al.,[12] with the cross section for reactions (1), (2), and (3). In Fig. 14 we give the ratio of the cross sections for production of the $\pi^+\pi^-n$ and $\pi^-p\pi^0$ final states as a function of energy. In these graphs we also include other measurements of the inelastic reactions.[13]

## IV. EXPERIMENTAL RESULTS

In this section we describe the properties of the two inelastic reactions and give representative distributions throughout our data. Preliminary analyses of these final states is left until the following section.

### A. Mass Squared Distributions

In Fig. 15 we show the Dalitz plots for the two inelastic channels at four energies within our range, while in Figs. 16 and 17 we give the corresponding projections (the origin of the curves in Fig. 16 is discussed in Section V). The major features of resonance production are apparent from these plots. At low energies there is copious $\pi\Delta(1238)$ production, Clebsch-Gordon coefficients favoring the production of $\Delta^-$ in the $I = 1/2$ component of the $\pi^+\pi^-n$ final state.[14] At higher energies $\rho N$ production becomes increasingly important, eventually dominating $\pi\Delta$ production.

At low energies the well known enhancement at high $\pi\pi$ masses is observed in the $\pi^+\pi^-n$ final state[15] but not in $\pi^-\pi^0p$.

From approximately 1700 MeV onwards the production of $\Delta^-$, particularly in the backward direction, falls rapidly (see Section V) as one might expect in the absence of exotic resonance contribution to the diagrams indicated in Fig. 18.

B. Production Angular Distributions

In Figs. 19 and 20 we show the production angular distributions of the three final state particles at the same c. m. energies. At lower energies the $\pi\pi N$ system is dominated by the decay of s-channel resonances leading to more symmetrical and iostropic distributions. However as the energy increases a peripheral nature of the reactions begins to emerge as characterized by the production angular distribution of the final nucleon. One other feature worth remarking on is the presence of the forward peak in the $\pi^+$ production angular distribution in the $\pi^+\pi^-n$ final state. If interpreted in terms of a t-channel effect (see Fig. 18) this would imply the presence of exotic exchange but it is probably due to the persistence of s-channel contributions. As remarked earlier the production cross section of the $\Delta^-$ is falling rapidly at the higher energies. This data has already been used to indicate an explanation of forward $\Delta^-$ production observed in the reaction[16, 17, 18]

$$p + n \longrightarrow \Delta^- \pi^+ p$$

C. Moments Analysis

A complete description of 3-particle final states in terms of angular and mass projections is impossible. A better description, though still not complete, is in terms of moments.[19, 20, 21, 22] To do this we express the angular distribution of the incident target proton in a coordinate system defined by the final state particles. We write

$$\frac{d\sigma}{d\Omega} = \sum_{LM} \left[\frac{2L+1}{4\pi}\right]^{1/2} B_L^M Y_L^{M*}(\theta, \phi) \qquad (4)$$

where $\theta$ and $\phi$ are the polar coordinates of the incident proton. Equation (4) can be rewritten as

$$\frac{1}{\sigma}\frac{d\sigma}{d\Omega} = \frac{1}{4\pi} + \sum_{\substack{L \geq 1 \\ M}} \left[\frac{2L+1}{4\pi}\right]^{1/2} \frac{B_L^M}{B_0^o} Y_L^{M*}(\theta, \phi)$$

$$= \frac{1}{4\pi} + \sum_{\substack{L \geq 1 \\ M}} \left[\frac{2L+1}{4\pi}\right]^{1/2} W_L^M Y_L^{M*}(\theta, \phi) \quad \ldots \qquad (4')$$

i.e., $W_0^o$ is normalized to unity.

In order to give a useful representation of the data we have calculated the moments $W_L^M$ for the following categories of events as a function of energy:

i) all data

ii) events lying within $1.140 < M(\pi^- n) < 1.320$ $(\pi^+\pi^- n)$

$1.140 < M(\pi^- p) < 1.320$ $(\pi^- p\pi^o)$

iii) events lying within $1.140 < M(\pi^+ n) < 1.320$ $(\pi^+\pi^- n)$

$1.140 < M(\pi^o p) < 1.320$ $(\pi^- pn^o)$

iv) events lying within $0.680 < M(\pi^+\pi^-) < 0.840$ $(\pi^+\pi^- n)$

$0.680 < M(\pi^-\pi^o) < 0.840$ $(\pi^- pn^o)$

So that the angular distributions are suitable for comparison with models for the production of $\Delta$ and $\rho$ resonances we have used a variety of coordinate systems. In all cases we have taken

$$\hat{OZ} = \vec{P}_{\pi^-} \times P_{\pi^+} \qquad (\pi^+\pi^- n)$$

$$\hat{OZ} = \vec{P}_{\pi^-} \times \vec{P}_{\pi o} \qquad (\pi^- p\pi^o)$$

but the definition of $\hat{OX}$ changes. These definitions are

i) and iv) $\qquad \hat{OX} = \vec{P}_N$

ii) $\hat{OX} = \vec{P}_{\pi^+}$ $(\pi^+\pi^- n)$

$\hat{OX} = \vec{P}_{\pi^0}$ $(\pi^- p\bar{n}^0)$

iii) $\hat{OX} = \vec{P}_{\pi^-}$ $(\pi^+\pi^- n)$

$\hat{OX} = \vec{P}_{\pi^-}$ $(\pi^- p\pi^0)$

The axis $\hat{OY}$ is then given by

$$\hat{OY} = \hat{OZ} \times \hat{OX}$$

$\vec{P}_N$, $\vec{P}_{\pi^-}$, $\vec{P}_\pi$ are the momenta of the 3 final state particles measured in the c.m. system.

Parity conservation[21,22] implies that

$$W_L^M = 0 \text{ if } L + M \text{ is odd.}$$

Interference of waves of the same parity contribute to those $W_L^M$ with L even, while interference of waves of opposite parity only give $W_L^M$ with L odd.[21,22]

In Figs. 21 - 28 we give the variation of these moments for $L \leq 5$ throughout the range of our data.[23] The data is available in tabular form elsewhere.[24] Moments for $L > 5$ are consistent with zero as are those moments forbidden by parity conservation.

A wave of total angular momentum j contributes to terms with $L \leq 2j-1$. In the region of ~1700 MeV $L = 4$ moments are nonzero due to the presence of the $D_{15}$ and $F_{15}$ resonances. However $L = 5$ moments, corresponding to the interference effects of these resonances, are consistent with zero indicating the presence of cancellations in the Dalitz plot. Even at the highest energies these moments indicate that only waves of $j \leq 5/2$ are necessary, but one should be careful in light of the cancellations we know can occur.

The structure in $W_1^1$ in the region of 1500 MeV we presume is due to interference between the $P_{11}$ and $D_{13}$ resonances. Indeed the large values of moments

with L odd indicate the presence of appreciable quantities of waves of opposite parities at all c.m. energies.

## V. INTERPRETATION AND ANALYSIS OF THE DISTRIBUTIONS

Two preliminary analyses of the data have been made: (i) an analysis of the Dalitz plot in the $\pi^-\pi^+n$ final state; (ii) a partial wave analysis of a subsample of events comprising the reaction

$$\pi^- p \rightarrow \pi^+ \Delta^-$$

in the region of the $F_{15}$ and $D_{15}$ resonances. This latter analysis has been presented elsewhere.[25]

(i) Analysis of the Dalitz plot in $\pi^+\pi^-n$ final state.

The Dalitz plot has been fitted using the maximum likelihood fitting program MURTLEBURT.[26] This uses an incoherent sum of processes to describe the reaction, the processes in this case being

$\pi^- p \rightarrow \pi^+ \Delta^-$

$\pi^- \Delta^+$

$\rho^0 n$ (only above a c.m.s. energy of 1600 MeV)

$\pi^+\pi^- n$ phase space

The resonance amplitudes are written in the form of a relativistic Breit-Wigner[27]

$$T = \Gamma_0 \omega_0 \left(\frac{\omega}{\omega_0}\right)\left(\frac{q_0}{q}\right) \frac{\omega_0 \Gamma(\omega)}{\left(\omega_0^2 - \omega^2\right) + \omega_0^2 \Gamma^2(\omega)} \quad . \; . \; . \qquad (5)$$

where

$$\Gamma(\omega) = \Gamma_0 \left(\frac{q}{q_0}\right)^{2L+1} \frac{B_L(qr)}{B_L(q_0 r)}$$

and

| | |
|---|---|
| $\omega$ | diparticle mass |
| $q$ | momentum in diparticle decay |
| $\omega_0$ | resonance mass |
| $q_0$ | momentum of particles when $\omega = \omega_0$ |
| $\Gamma_0$ | width of the resonance at $\omega = \omega_0$ |
| $\Gamma$ | decay width at mass $\omega$ |
| $B_L(qr)$ | barrier penetration factor[28] |
| $L$ | orbital angular momentum in the decay of the resonance |

The factors present in (5) normalize the amplitude at resonance to unity. We use the following values for the masses and widths of the resonances in the fit.

$$M(\Delta) = 1236 \text{ MeV} \qquad \Gamma_0(\Delta) = 130 \text{ MeV}$$

$$M(\rho) = 765 \text{ MeV} \qquad \Gamma_0(\rho) = 130 \text{ MeV}$$

The fractions of the various resonance and phase space contributions determined by this method are given in Table IV and Fig. 29. The quality of the fits can be seen by inspecting Fig. 16 where the curves are derived from the final fits. Below a c.m.s. energy of 1496 MeV no fits were obtained due to the large overlap of the $\Delta$ bands in the Dalitz plot. The steady decrease in the fraction of $\Delta^-$ is apparent together with the rapid increase in $\rho^0$ production from threshold.

A similar attempt to fit the $\pi^-\pi^0 p$ final state was inconclusive; presumably because the incoherent sum of the amplitudes for the various processes cannot describe the final state.

(ii) <u>Partial wave analysis of $\pi^- p \rightarrow \pi^+ \Delta^-$ in the c.m.s. energy range 1647-1766 MeV.</u>

The analysis of this reaction has been described elsewhere[25] and we present only a summary of the conclusions here.

The production angular distribution and cross sections for the reaction were fitted using the partial wave analysis described by A. Brody and A. Kernan.[29] The partial wave amplitudes used were (the notation employed is L, 2J where L is the $\pi\Delta$ orbital angular momentum and J the total angular momentum)

1) P5 containing the $F_{15}$ resonance

   D5 containing the $D_{15}$ resonance

2) S3, P1, D1, F7 containing background amplitudes.

The resonances are described by Breit-Wigner shapes and the backgrounds are parameterized as linear functions of the c.m.s. momentum.

In the analysis two solutions, A and B, were found. The $F_{15}$ and $D_{15}$ resonance parameters corresponding to these solutions are given in Table V, while the variations of the resonant amplitudes and the background amplitudes are shown in Fig. 30. In Fig. 31 we display the fits to the production angular distributions at all energy points in our analysis and in Fig. 32 we give the contributions of the individual waves to the cross section.

## VI. DISCUSSION OF RESULTS

The interpretation of the single pion production data is exceedingly complicated. The analyses described here are only a beginning and more sophisticated approaches are required.[13,21,22] At present we are pursuing an analysis (within the spirit of isobar model) using a maximum likelihood fit to the data. Such analyses require large quantities of time and we felt it worthwhile to present the experimental data at an earlier stage. Only when this analysis is complete will we begin to have a description of the $\pi\pi N$ final state.

However, even the experimental presentation of 3-body final states presents many problems which we do not pretend to have surmounted. In the future we hope

to have available magnetic tapes containing the experimental information, this being the only solution to these problems.

## VII. ACKNOWLEDGEMENTS

We would like to thank F. S. Crawford Jr., and J. A. Anderson for making available the LRL HBC flim. We also wish to thank the LRL Spiral Reader crew and especially G. R. Lynch and L. J. Lloyd for their help and assistance in measuring the film, and the SLAC CDA staff for their scanning effort. Finally, we wish to acknowledge the valuable assistance at the early stage of the experiment of R. Diebold.

## REFERENCES


1. P. Bareyre, C. Bricman, A. V. Stirling and G. Villet, Phys. Letters 18, 342 (1965); P. Bareyre, C. Bricman and G. Villet, Phys. Rev. 165, 1730 (1968).
2. B. H. Bransden, P. J. O'Donnell and R. G. Moorhouse, Phys. Letters 11, 339 (1964); Phys. Rev. 139B, 1566 (1965); Proc. Roy. Soc. (London) A289, 538 (1966); Phys. Letters 19, 420 (1965).
3. P. Auvil, A. Donnachie, A. T. Lea, and C. Lovelace, Phys. Letters 12, 76 (1964); 19, 148 (1965).
4. L. D. Roper, Phys. Rev. Letters 12, 340 (1964); L. D. Roper, R. M. Wright, and B. T. Feld, Phys. Rev. 138B, 190 (1965); L. D. Roper and R. M. Wright, Phys. Rev. 138B, 921 (1965).
5. R. J. Cence, Phys. Letters 20, 306 (1966).
6. C. H. Johnson, UCRL-17683 (1967).
7. A. Donnachie, R. G. Kirsopp, and C. Lovelace, Phys. Letters 26B, 161 (1968); C. Lovelace, Proceedings of the 1967 Heidelberg Conference (North Holland Publishing Co., Amsterdam, 1967), p. 79, H. Filthuth, ed.; C. Lovelace in Proceedings of the Conference on $\pi$N Scattering, Irvine, California, 1967, edited by G. L. Shaw and D. Y. Wong (Wiley, New York, 1967); CERN Preprint TH-839 (1967).
8. R. G. Moorhouse, Ann. Rev. Nucl. Sci. 19, 301 (1969).
9. R. J. Plano, Proceedings of the Lund International Conference on Elementary Particles, July 1969, p. 313, G. von Dardel, editor.
10. A. D. Brody, R. J. Cashmore, A. Kernan, D.W.G.S. Leith, B. S. Levi, B. C. Shen, J. P. Berge, D. J. Herndon, L. R. Price, A. H. Rosenfeld, P. Soding, "$\pi^-$p elastic scattering in the CMS energy range 1400-2000 MeV," to be published in Phys. Rev.

11. Due to variations in the reliability of the pulse height information from the Spiral Reader it is necessary, in constructing $\chi^2_{comb}$, to introduce a factor $\alpha$ which reflects this fact. Thus we used

$$\chi^2_{comb} = \chi^2_K + \alpha \chi^2_{ion}$$

where $\alpha = 2.0/\langle\chi^2_{ion}\rangle$ and $\langle\chi^2_{ion}\rangle$ was determined from 100 unambiguous inelastic events at a time. $\alpha$ varied from 0.8 to 0.25.

12. A. A. Carter, K. F. Riley, R. J. Tapper, D. V. Bugg, R. S. Gilmore, K. M. Knight, D. C. Salter, G. H. Stafford, E.J.N. Wilson, J. D. Davies, J. D. Dowell, P. M. Hattersley, R. J. Homer, and A. W. O'Dell, Phys. Rev. 168, 1457 (1968).

13. M. De Beer, B. Deler, J. Dolbeau, M. Neveu, Nguyen Thuc Diem, G. Smadja, and G. Valladas, Nucl. Phys. B12, 599 (1969); W. Chinowsky, J. H. Mulvey, and D. H. Saxon, Phys. Rev. 2D, 1790 (1970).

14. $\pi\Delta$ production in different isospin states leads to the following ratios (neglecting any interference effects)

| | | | | | |
|---|---|---|---|---|---|
| I = 1/2 | $\pi^+\pi^-n$; | $\frac{\Delta^-}{\Delta^+} = \frac{9}{1}$ | $\pi^-\pi^0p$; | $\frac{\Delta^0}{\Delta^+} = \frac{2}{2}$; | $\frac{\pi^+\pi^-n}{\pi^-\pi^0p} = \frac{10}{4}$ |
| I = 3/2 | $\pi^+\pi^-n$; | $\frac{\Delta^-}{\Delta^+} = \frac{18}{8}$ | $\pi^-\pi^0p$; | $\frac{\Delta^0}{\Delta^+} = \frac{1}{16}$; | $\frac{\pi^+\pi^-n}{\pi^-\pi^0p} = \frac{26}{17}$ |

$\rho N$ production in different isospin states leads to the following ratios

I = 1/2 $\quad \frac{\pi^+\pi^-n}{\pi^-\pi^0p} = \frac{1}{2}$

I = 3/2 $\quad \frac{\pi^+\pi^-n}{\pi^-\pi^0p} = \frac{2}{1}$

15. J. Kirz, J. Schwarz and R. D. Tripp, Phys. Rev. 130, 2481 (1963).

16. H. O. Cohn, R. D. McCulloch, W. M. Bugg, and G. T. Conde, Phys. Letters 26B, 598 (1969).

17. G. Yekutieli, D. Yaffe, S. Toaff, A. Shapira, E. E. Ronat, U. Karson, B. Haber and Y. Eisenberg, Phys. Rev. Letters 25, 184 (1970).

18. E. L. Berger and R. A. Morrow, Phys. Rev. Letters 25, 1136 (1970).

19. D. Branson, P. V. Landshoff and J. C. Taylor, Phys. Rev. 132, 902 (1962).

20. R. C. Arnold and J. L. Uretsky, Phys. Rev. 153, 1443 (1967).

21. D. H. Morgan, Phys. Rev. 166, 1731 (1968).

22. R. J. Cashmore, D. Phil. Thesis, Oxford University, England (unpublished).

23. We only give moments for $M \geq 0$. Other values may be obtained using the relation

$$W_L^{-M} = (-1)^M W_L^{M*}.$$

24. A. D. Brody, R. J. Cashmore, A. Kernan, D.W.G.S. Leith, B. G. Levi, A. Minten, B. C. Shen, J. P. Berge, B. Deler, D. J. Herndon, R. Longacre, L. R. Miller, L. R. Price, A. Rosenfeld, P. Soding, Report No. SLAC-PUB-911, Supplement 1.

25. A. D. Brody, R. J. Cashmore, A. Kernan, D.W.G.S. Leith, B. G. Levi, B. C. Shen, D. J. Herndon, L. R. Price, A. H. Rosenfeld, P. Soding, "The reaction $\pi^- p \rightarrow \pi^+ \Delta^-$ at c.m. energies 1640-1760 MeV," Phys. Letters 34B, 665 (1971).

26. Murtleburt, J. Friedman, Lawrence Radiation Laboratory, Berkeley, Alvarez Programming Group Note No. P-156, unpublished.

27. J. D. Jackson, Nuovo Cimento 34, 1644 (1964).

28. J. M. Blatt and V. F. Weisskopf, Theoretical Nuclear Physics (John Wiley and Sons, Inc., New York, 1956).

29. A. D. Brody and A. Kernan, Phys. Rev. 182, 1785 (1969).

TABLE I

Events Processed at Each Energy

| Exposure | $E_{c.m.}$ (MeV) | $p_{lab}^{\pi^-}$ (MeV/c) | 4-C Events $\chi^2 \leq 14$ | 1-C $n\pi\pi$ Events $\chi^2 \leq 8$ | 1-C $p\pi\pi$ Events $\chi^2 \leq 8$ |
|---|---|---|---|---|---|
| 30" HBC(I) | 1406 | 556 | 648 | 255 | 80 |
| | 1440 | 609 | 500 | 215 | 82 |
| | 1472 | 660 | 1110 | 418 | 245 |
| | 1496 | 699 | 1854 | 675 | 499 |
| | 1527 | 750 | 2337 | 832 | 701 |
| | 1556 | 797 | 826 | 340 | 272 |
| | 1589 | 853 | 997 | 579 | 387 |
| | 1709 | 1067 | 1141 | 585 | 400 |
| | 1730 | 1105 | 1954 | 1046 | 836 |
| | 1762 | 1165 | 2230 | 1231 | 899 |
| 30" HBC(II) | 1811 | 1259 | 1544 | 1096 | 651 |
| | 1843 | 1322 | 2777 | 2172 | 1337 |
| | 1872 | 1381 | 2920 | 2443 | 1568 |
| | 1904 | 1444 | 3160 | 2616 | 1694 |
| | 1935 | 1509 | 1606 | 1288 | 886 |
| 30" HBC(III) | 1720 | 1084 | 687 | 392 | 262 |
| | 1761 | 1161 | 1200 | 786 | 488 |
| | 1787 | 1212 | 1210 | 798 | 476 |
| | 1806 | 1250 | 292 | 188 | 122 |
| | 1821 | 1278 | 1740 | 1098 | 687 |
| | 1853 | 1340 | 2213 | 1649 | 979 |
| | 1885 | 1404 | 2392 | 1970 | 1180 |
| | 1916 | 1469 | 3792 | 3203 | 2105 |
| | 1933 | 1503 | 1972 | 1735 | 1177 |
| | 1963 | 1567 | 4113 | 3512 | 2405 |
| | 1980 | 1602 | 3957 | 3416 | 2458 |
| | | | | $\chi^2 \leq 7$ | $\chi^2 \leq 7$ |
| 72" HBC | 1628 | 924 | 537 | 358 | 200 |
| | 1647 | 956 | 5482 | 3169 | 1968 |
| | 1660 | 979 | 2697 | 1430 | 879 |
| | 1669 | 995 | 5127 | 2562 | 1603 |
| | 1674 | 1004 | 4966 | 2673 | 1568 |
| | 1685 | 1024 | 4398 | 2281 | 1409 |
| | 1695 | 1042 | 2206 | 1299 | 871 |
| | 1740 | 1125 | 3594 | 2259 | 1786 |
| | 1766 | 1174 | 1733 | 1120 | 854 |
| TOTALS | | | 79,911 | 51,477 | 33,880 |

1801839

TABLE II

Azimuthal Correction Factors and Errors

| C.M.S. Energy | $\pi^+\pi^-n$ | | $\pi^-\pi^0p$ | |
|---|---|---|---|---|
| | Correction | Error | Correction | Error |
| 1406 | 1.09 | 0.10 | 1.00 | 0.15 |
| 1440 | 1.08 | 0.10 | 1.00 | 0.15 |
| 1471 | 1.15 | 0.09 | 1.07 | 0.08 |
| 1496 | 1.15 | 0.06 | 1.06 | 0.06 |
| 1527 | 1.10 | 0.06 | 1.01 | 0.05 |
| 1556 | 1.08 | 0.09 | 1.08 | 0.09 |
| 1589 | 1.08 | 0.07 | 1.05 | 0.07 |
| 1629 | 1.09 | 0.07 | 1.05 | 0.09 |
| 1647 | 1.03 | 0.02 | 1.02 | 0.03 |
| 1660 | 1.05 | 0.03 | 1.01 | 0.04 |
| 1669 | 1.04 | 0.02 | 1.01 | 0.03 |
| 1674 | 1.10 | 0.03 | 1.03 | 0.03 |
| 1685 | 1.08 | 0.03 | 1.00 | 0.03 |
| 1695 | 1.07 | 0.04 | 1.06 | 0.05 |
| 1709 | 1.07 | 0.06 | 1.10 | 0.09 |
| 1720 | 1.05 | 0.07 | 1.08 | 0.10 |
| 1730 | 1.12 | 0.05 | 1.03 | 0.05 |
| 1740 | 1.05 | 0.03 | 1.05 | 0.03 |
| 1761 | 1.10 | 0.06 | 1.00 | 0.06 |
| 1762 | 1.07 | 0.05 | 1.00 | 0.04 |
| 1766 | 1.02 | 0.04 | 1.02 | 0.04 |
| 1787 | 1.03 | 0.05 | 1.02 | 0.07 |
| 1806 | 1.00 | 0.09 | 1.00 | 0.11 |
| 1811 | 1.05 | 0.04 | 1.02 | 0.05 |
| 1821 | 1.04 | 0.04 | 1.02 | 0.05 |
| 1843 | 1.05 | 0.03 | 1.01 | 0.03 |
| 1853 | 1.01 | 0.03 | 1.03 | 0.05 |
| 1873 | 1.08 | 0.04 | 1.00 | 0.03 |
| 1884 | 1.07 | 0.04 | 1.00 | 0.04 |
| 1904 | 1.01 | 0.03 | 1.02 | 0.03 |
| 1916 | 1.06 | 0.03 | 1.02 | 0.03 |
| 1932 | 1.08 | 0.04 | 1.04 | 0.04 |
| 1935 | 1.03 | 0.04 | 1.05 | 0.05 |
| 1963 | 1.07 | 0.03 | 1.02 | 0.03 |
| 1980 | 1.06 | 0.03 | 1.02 | 0.03 |

1801829

TABLE III

Cross Sections

| C.M.S. Energy | $\pi^- p \to \pi^- p$ | | $\pi^- p \to \pi^- \pi^+ n$ | | $\pi^- p \to \pi^- \pi^0 p$ | |
|---|---|---|---|---|---|---|
| | $\sigma$(mb) | $\delta\sigma$(mb) | $\sigma$(mb) | $\delta\sigma$(mb) | $\sigma$(mb) | $\delta\sigma$(mb) |
| 1406 | 10.24 | 0.62 | 3.67 | 0.46 | 1.06 | 0.21 |
| 1440 | 12.86 | 0.94 | 4.79 | 0.62 | 1.69 | 0.33 |
| 1471 | 15.32 | 0.80 | 5.25 | 0.55 | 2.86 | 0.32 |
| 1496 | 19.07 | 0.74 | 5.84 | 0.47 | 3.98 | 0.35 |
| 1527 | 19.91 | 0.71 | 6.12 | 0.47 | 4.74 | 0.35 |
| 1556 | 14.91 | 0.96 | 5.30 | 0.60 | 4.24 | 0.49 |
| 1589 | 14.47 | 0.84 | 6.83 | 0.64 | 4.44 | 0.44 |
| 1629 | 18.80 | 1.32 | 12.38 | 1.47 | 6.66 | 0.93 |
| 1647 | 21.62 | 0.46 | 10.10 | 0.47 | 6.21 | 0.33 |
| 1660 | 23.16 | 0.66 | 10.47 | 0.64 | 6.19 | 0.43 |
| 1669 | 26.42 | 0.58 | 10.76 | 0.50 | 6.54 | 0.35 |
| 1674 | 24.22 | 0.54 | 10.92 | 0.54 | 6.00 | 0.32 |
| 1685 | 26.30 | 0.75 | 12.17 | 0.69 | 6.96 | 0.42 |
| 1695 | 26.01 | 0.86 | 11.45 | 0.77 | 7.60 | 0.58 |
| 1709 | 23.65 | 1.10 | 9.46 | 0.83 | 6.65 | 0.73 |
| 1720 | 19.48 | 1.35 | 9.33 | 1.06 | 6.41 | 0.87 |
| 1730 | 17.95 | 0.74 | 8.07 | 0.59 | 5.93 | 0.46 |
| 1740 | 18.29 | 0.47 | 7.64 | 0.40 | 6.04 | 0.32 |
| 1761 | 13.66 | 0.78 | 7.56 | 0.74 | 4.26 | 0.45 |
| 1762 | 15.01 | 0.50 | 6.49 | 0.47 | 4.43 | 0.31 |
| 1766 | 15.73 | 0.61 | 7.95 | 0.61 | 6.06 | 0.47 |
| 1787 | 12.45 | 0.59 | 6.92 | 0.55 | 4.09 | 0.40 |
| 1806 | 13.31 | 1.08 | 7.22 | 0.98 | 4.68 | 0.75 |
| 1811 | 13.80 | 0.61 | 8.30 | 0.64 | 4.79 | 0.41 |
| 1821 | 12.80 | 0.55 | 6.76 | 0.47 | 4.15 | 0.33 |
| 1843 | 13.09 | 0.45 | 8.33 | 0.54 | 4.93 | 0.34 |
| 1853 | 12.38 | 0.45 | 7.40 | 0.50 | 4.48 | 0.36 |
| 1873 | 12.53 | 0.39 | 8.73 | 0.55 | 5.19 | 0.32 |
| 1884 | 12.34 | 0.50 | 8.68 | 0.67 | 4.86 | 0.39 |
| 1904 | 11.95 | 0.36 | 7.84 | 0.47 | 5.13 | 0.31 |
| 1916 | 10.87 | 0.36 | 7.31 | 0.45 | 4.62 | 0.30 |
| 1932 | 11.69 | 0.49 | 7.97 | 0.61 | 5.21 | 0.41 |
| 1935 | 10.39 | 0.47 | 6.76 | 0.58 | 4.74 | 0.44 |
| 1963 | 10.21 | 0.29 | 7.43 | 0.42 | 4.85 | 0.28 |
| 1980 | 9.82 | 0.33 | 6.36 | 0.36 | 4.40 | 0.26 |

1801830

TABLE IV

Fractions of Resonance and Phase Space Production in the Reaction $\pi^- p \rightarrow \pi^+ \pi^- n$

| C.M.S. Energy | $\Delta^-$ | $\Delta^+$ | $\rho^0$ | Phase Space |
|---|---|---|---|---|
| 1496 | 0.529 ± 0.087 | 0.052 ± 0.079 | 0. | 0.419 ± 0.118 |
| 1527 | 0.500 ± 0.069 | 0.187 ± 0.066 | 0. | 0.313 ± 0.095 |
| 1556 | 0.565 ± 0.086 | 0.337 ± 0.082 | 0. | 0.098 ± 0.119 |
| 1589 | 0.639 ± 0.056 | 0.157 ± 0.050 | 0. | 0.204 ± 0.075 |
| 1629 | 0.357 ± 0.072 | 0.017 ± 0.064 | 0.091 ± 0.049 | 0.535 ± 0.108 |
| 1647 | 0.551 ± 0.024 | 0.036 ± 0.020 | 0.011 ± 0.015 | 0.402 ± 0.035 |
| 1660 | 0.545 ± 0.035 | 0.051 ± 0.030 | 0.003 ± 0.021 | 0.401 ± 0.045 |
| 1669 | 0.535 ± 0.026 | 0.025 ± 0.021 | 0.010 ± 0.016 | 0.430 ± 0.037 |
| 1674 | 0.537 ± 0.026 | 0.016 ± 0.021 | 0.031 ± 0.015 | 0.416 ± 0.037 |
| 1685 | 0.576 ± 0.027 | 0.072 ± 0.023 | 0.003 ± 0.016 | 0.349 ± 0.039 |
| 1695 | 0.554 ± 0.036 | 0.006 ± 0.029 | 0.004 ± 0.020 | 0.564 ± 0.050 |
| 1709 | 0.440 ± 0.068 | 0.000 ± 0.052 | 0.011 ± 0.034 | 0.451 ± 0.092 |
| 1720 | 0.590 ± 0.064 | 0.114 ± 0.055 | 0.000 ± 0.037 | 0.296 ± 0.092 |
| 1730 | 0.452 ± 0.039 | 0.001 ± 0.031 | 0.082 ± 0.025 | 0.465 ± 0.056 |
| 1740 | 0.569 ± 0.026 | 0.075 ± 0.020 | 0.057 ± 0.017 | 0.299 ± 0.037 |
| 1761 | 0.590 ± 0.043 | 0.111 ± 0.036 | 0.097 ± 0.030 | 0.202 ± 0.064 |
| 1762 | 0.431 ± 0.036 | 0.096 ± 0.030 | 0.108 ± 0.025 | 0.365 ± 0.052 |
| 1766 | 0.348 ± 0.038 | 0.000 ± 0.028 | 0.225 ± 0.027 | 0.427 ± 0.054 |
| 1787 | 0.412 ± 0.044 | 0.087 ± 0.034 | 0.173 ± 0.033 | 0.328 ± 0.065 |
| 1806 | 0.363 ± 0.082 | 0.056 ± 0.068 | 0.278 ± 0.071 | 0.303 ± 0.128 |
| 1811 | 0.330 ± 0.034 | 0.081 ± 0.028 | 0.231 ± 0.029 | 0.358 ± 0.053 |
| 1821 | 0.279 ± 0.034 | 0.006 ± 0.026 | 0.293 ± 0.029 | 0.422 ± 0.053 |
| 1843 | 0.245 ± 0.023 | 0.045 ± 0.019 | 0.307 ± 0.029 | 0.403 ± 0.042 |
| 1853 | 0.250 ± 0.025 | 0.069 ± 0.022 | 0.337 ± 0.024 | 0.344 ± 0.041 |
| 1873 | 0.179 ± 0.020 | 0.042 ± 0.017 | 0.364 ± 0.020 | 0.413 ± 0.033 |
| 1884 | 0.249 ± 0.022 | 0.030 ± 0.017 | 0.411 ± 0.022 | 0.310 ± 0.035 |
| 1904 | 0.184 ± 0.018 | 0.079 ± 0.017 | 0.377 ± 0.020 | 0.360 ± 0.032 |
| 1916 | 0.174 ± 0.016 | 0.057 ± 0.014 | 0.424 ± 0.018 | 0.345 ± 0.028 |
| 1932 | 0.149 ± 0.021 | 0.061 ± 0.019 | 0.412 ± 0.024 | 0.378 ± 0.037 |
| 1935 | 0.154 ± 0.024 | 0.109 ± 0.023 | 0.404 ± 0.028 | 0.333 ± 0.043 |
| 1973 | 0.142 ± 0.014 | 0.075 ± 0.013 | 0.426 ± 0.017 | 0.357 ± 0.026 |
| 1980 | 0.125 ± 0.087 | 0.087 ± 0.013 | 0.426 ± 0.017 | 0.362 ± 0.090 |

1801B42

TABLE V

$F_{15}$ and $D_{15}$ Resonance Parameters from a Partial Wave Analysis of the Reaction $\pi^- p \rightarrow \Delta^- \pi^+$

| Resonance | Parameter | Solution A | Solution B |
|---|---|---|---|
| $F_{15}$ | Mass | $1.690 \pm 0.005$ | $1.686 \pm .009$ |
| | Width | $0.077 \pm 0.022$ | $0.130^{+0.035}_{-0.053}$ |
| | $\Delta\pi$ branching fraction | $0.13^{+0.03}_{-0.04}$ | $0.39^{+0.06}_{-0.10}$ |
| $D_{15}$ | Mass | $1.671 \pm 0.004$ | $1.680 \pm 0.009$ |
| | Width | $0.112 \pm 0.017$ | $0.158^{+0.090}_{-0.020}$ |
| | $\Delta\pi$ branching fraction | $0.63 \pm 0.07$ | $0.63^{+0.07}_{-0.11}$ |
| Relative sign of $D_{15}$ and $F_{15}$ coupling to $\Delta\pi$ | | - | + |

## FIGURE CAPTIONS

1. Beam track pull quantities in the reaction $\pi^- p \rightarrow \pi^- \pi^+ n$. The shaded area corresponds to ±1.

2. Beam track pull quantities in the reaction $\pi^- p \rightarrow \pi^- \pi^0 p$. The shaded area corresponds to ±1.

3. Chisquare distributions for the reaction $\pi^- p \rightarrow \pi^- \pi^+ n$. The value of $\chi^2_{comb}$ is discussed in Section II.

4. Chisquare distributions for the reaction $\pi^- p \rightarrow \pi^- \pi^0 p$. The value of $\chi^2_{comb}$ is discussed in Section II.

5. Missing mass distributions for the reactions $\pi^- p \rightarrow \pi^- \pi^+ n$ and $\pi^- p \rightarrow \pi^- \pi^0 p$.

6. Missing mass distributions for ambiguous events assigned to the reaction $\pi^- p \rightarrow \pi^- \pi^+ n$.

7. Missing mass distributions for ambiguous events assigned to the reaction $\pi^- p \rightarrow \pi^- \pi^0 p$.

8. Chisquare distribution for ambiguous events assigned to the reaction $\pi^- p \rightarrow \pi^- \pi^+ n$ when interpreted as being $\pi^- p \rightarrow \pi^- \pi^0 p$.

9. Chisquare distribution for ambiguous events assigned to the reaction $\pi^- p \rightarrow \pi^- \pi^0 p$ when interpreted as being $\pi^- p \rightarrow \pi^- \pi^+ n$.

10. (a) Azimuthal correction factors as a function of CMS energy for the reaction $\pi^- p \rightarrow \pi^- \pi^+ n$.

    (b) Azimuthal correction factors as a function of CMS energy for the reaction $\pi^- p \rightarrow \pi^- \pi^0 p$.

    The numerical values for these quantities are given in Table II.

11. Cross sections for the reaction $\pi^- p \rightarrow \pi^- \pi^+ n$.

12. Cross sections for the reaction $\pi^- p \rightarrow \pi^- \pi^0 p$.

13. Cross section for the reactions $\pi^- p \rightarrow \pi^- p$, $\pi^- p \rightarrow \pi^- \pi^+ n$, $\pi^- p \rightarrow \pi^- \pi^0 p$, compared with the total cross section measurements of A. A. Carter et al.[11]

14. Ratio $\sigma(\pi^+\pi^-n)/\sigma(\pi^-\pi^0p)$ as a function of energy.

15. Dalitz plots for the reactions $\pi^-p \rightarrow \pi^-\pi^+n$, $\pi^-p \rightarrow \pi^-\pi^0p$.

16. Mass squared projections of the Dalitz plot in the final state $\pi^-p \rightarrow \pi^-\pi^+n$. The curves are from maximum likelihood fits to the Dalitz plot.

17. Mass squared projections of the Dalitz plot in the final state $\pi^-p \rightarrow \pi^-\pi^0p$.

18. Diagram for the production of forward $\pi^+$ mesons in the reaction $\pi^-p \rightarrow \pi^+\Delta^-$.

19. Production angular distributions of each particle in the final state $\pi^-p \rightarrow \pi^+\pi^-n$.

20. Production angular distributions of each particle in the final state $\pi^-p \rightarrow \pi^-\pi^0p$.

21. The moments $W_L^M$ as a function of energy in the final state $\pi^-\pi^+n$ normalized such that $W_0^0=1$ (see Eq. (4')). The x-axis is defined as $\vec{P}_n$, and the z-axis as $\vec{P}_{\pi^-} \times \vec{P}_{\pi^+}$.

22. The moments $W_L^M$ as a function of energy in the final state $\pi^-\pi^+n$ for $1140 < M(\pi^-n) < 1320$ MeV normalized such that $W_0^0=1$ (see Eq. (4')). The x-axis is defined as $\vec{P}_{\pi^+}$ and the z-axis as $\vec{P}_{\pi^-} \times \vec{P}_{\pi^+}$.

23. The moments $W_L^M$ as a function of energy in the final state $\pi^-\pi^+n$ for $1140 < M(\pi^+n) < 1320$ MeV normalized such that $W_0^0=1$ (see Eq. (4')). The x-axis is defined as $\vec{P}_{\pi^-}$ and the z-axis as $\vec{P}_{\pi^-} \times \vec{P}_{\pi^+}$.

24. The moments $W_L^M$ as a function of energy in the final state $\pi^-\pi^+n$ for $680 < M(\pi^-\pi^+) < 840$ MeV normalized such that $W_0^0=1$ (see Eq. (4')). The x-axis is defined as $\vec{P}_n$ and the z-axis as $\vec{P}_{\pi^-} \times \vec{P}_{\pi^+}$.

25. The moments $W_L^M$ as a function of energy in the final state $\pi^-\pi^0p$ normalized such that $W_0^0=1$ (see Eq. (4')). The x-axis is defined as $\vec{P}_p$ and the z-axis as $\vec{P}_{\pi^-} \times \vec{P}_{\pi^0}$.

26. The moments $W_L^M$ as a function of energy in the final state $\pi^-\pi^0p$ for $1140 < (M\pi^-p) < 1320$ MeV normalized such that $W_0^0=1$ (see Eq. (4')). The x-axis is defined as $\vec{P}_{\pi^0}$ and the z-axis as $\vec{P}_{\pi^-} \times \vec{P}_{\pi^0}$.

27. The moments $W_L^M$ as a function of energy in the final state $\pi^-\pi^o p$ for $1140 < M(\pi^o p) < 1320$ MeV normalized such that $W_0^o=1$ (see Eq. (4')). The x-axis is defined as $\vec{P}_{\pi^-}$ and the z-axis as $\vec{P}_{\pi^-} \times \vec{P}_{\pi^o}$.

28. The moments $W_L^M$ as a function of energy in the final state $\pi^-\pi^o p$ for $680 < M(\pi^-\pi^o) < 840$ MeV normalized such that $W_0^o=1$ (see Eq. (4')). The x-axis is defined as $\vec{P}_p$ and the z-axis as $\vec{P}_{\pi^-} \times \vec{P}_{\pi^o}$.

29. The fractions of resonance and phase space production in the reaction $\pi^- p \rightarrow \pi^-\pi^+ n$.

30. Variation of the partial wave amplitudes in two solutions A and B, resulting from fits[21] to the reaction $\pi^- p \rightarrow \pi^+ \Delta^-$.

31. Fits to the production angular distributions of the $\pi^+$ in the reaction $\pi^- p \rightarrow \pi^+ \Delta^-$ in solutions A and B.[21]

32. The experimental $\pi^+\pi^- n$ cross section ($1140\ \mathrm{MeV/c^2} < M(\pi^- n) < 1320\ \mathrm{MeV/c^2}$) together with the contributions of the various partial waves in solutions A and B.[21]

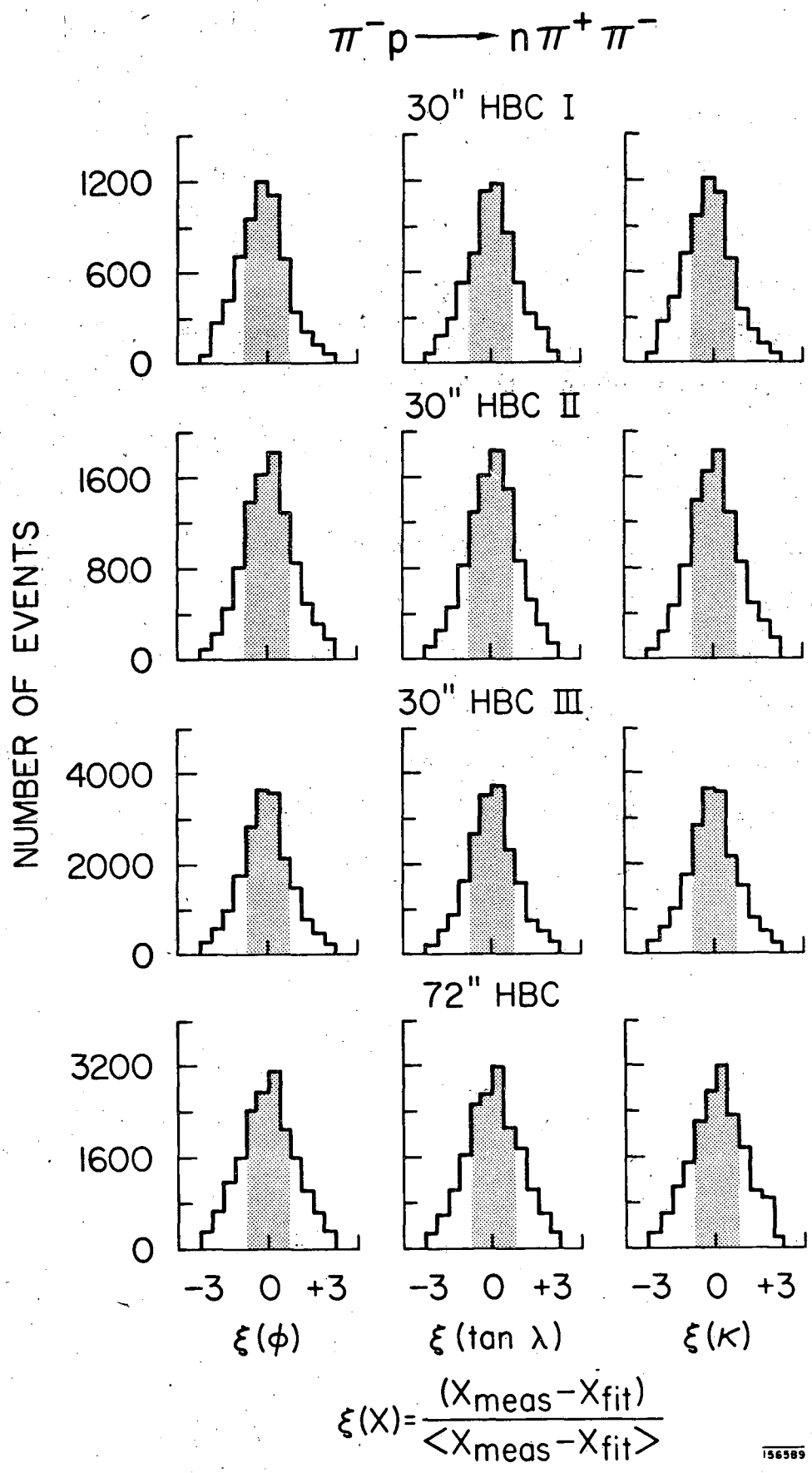
$\pi^- p \longrightarrow n\pi^+\pi^-$
30" HBC I
30" HBC II
30" HBC III
72" HBC
NUMBER OF EVENTS
1200
600
0
1600
800
0
4000
2000
0
3200
1600
0
−3 0 +3
ξ(φ)
ξ(tan λ)
ξ(κ)
$\xi(X) = \frac{(X_{meas} - X_{fit})}{\langle X_{meas} - X_{fit} \rangle}$
156589

Fig. 1

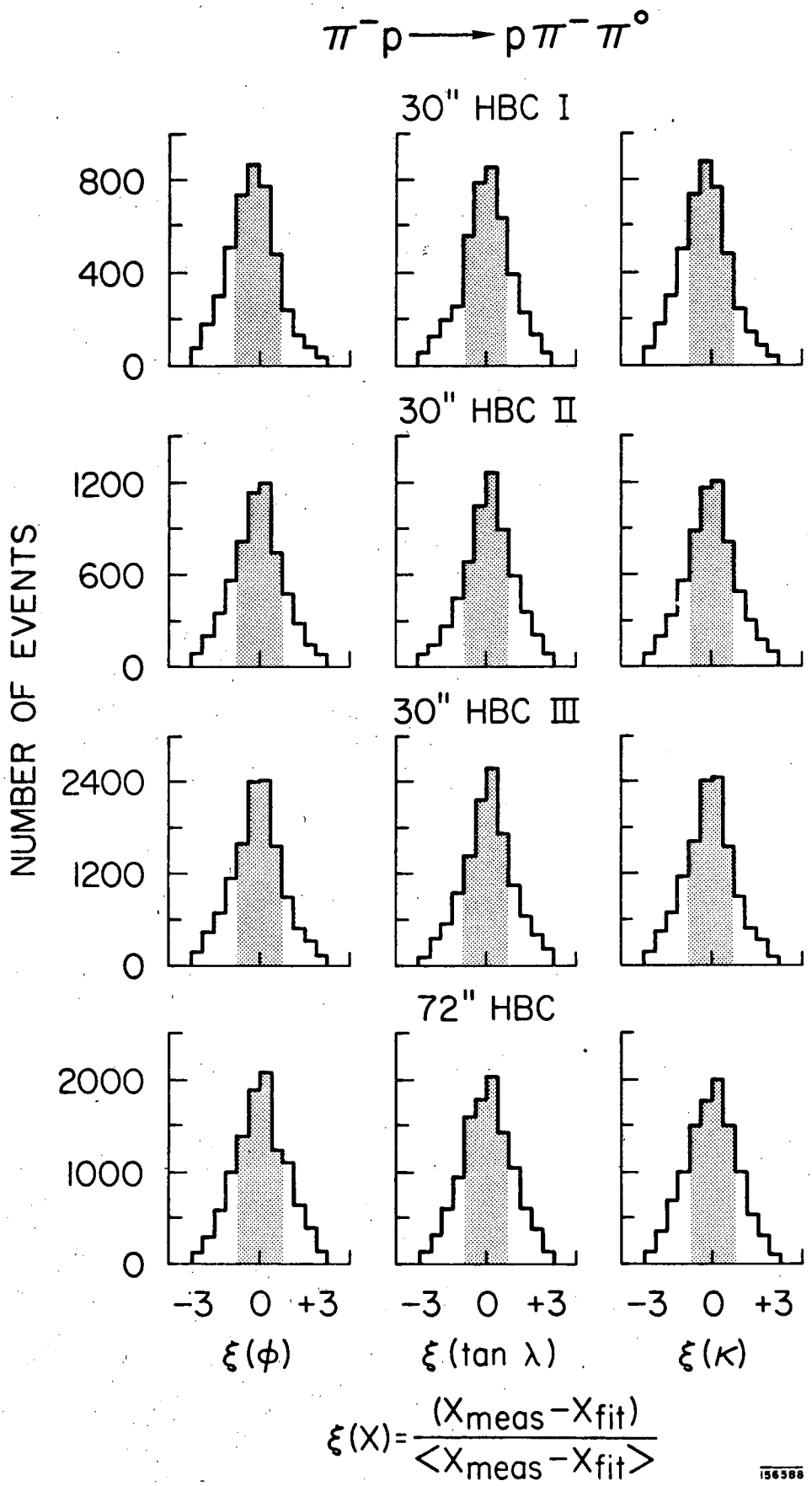
$\pi^- p \longrightarrow p \pi^- \pi^0$
30" HBC I
30" HBC II
30" HBC III
72" HBC
NUMBER OF EVENTS
800
400
0
1200
600
0
2400
1200
0
2000
1000
0
−3 0 +3
$\xi(\phi)$
$\xi(\tan\lambda)$
$\xi(\kappa)$
$\xi(X) = \frac{(X_{meas} - X_{fit})}{\langle X_{meas} - X_{fit} \rangle}$
156588

Fig. 2

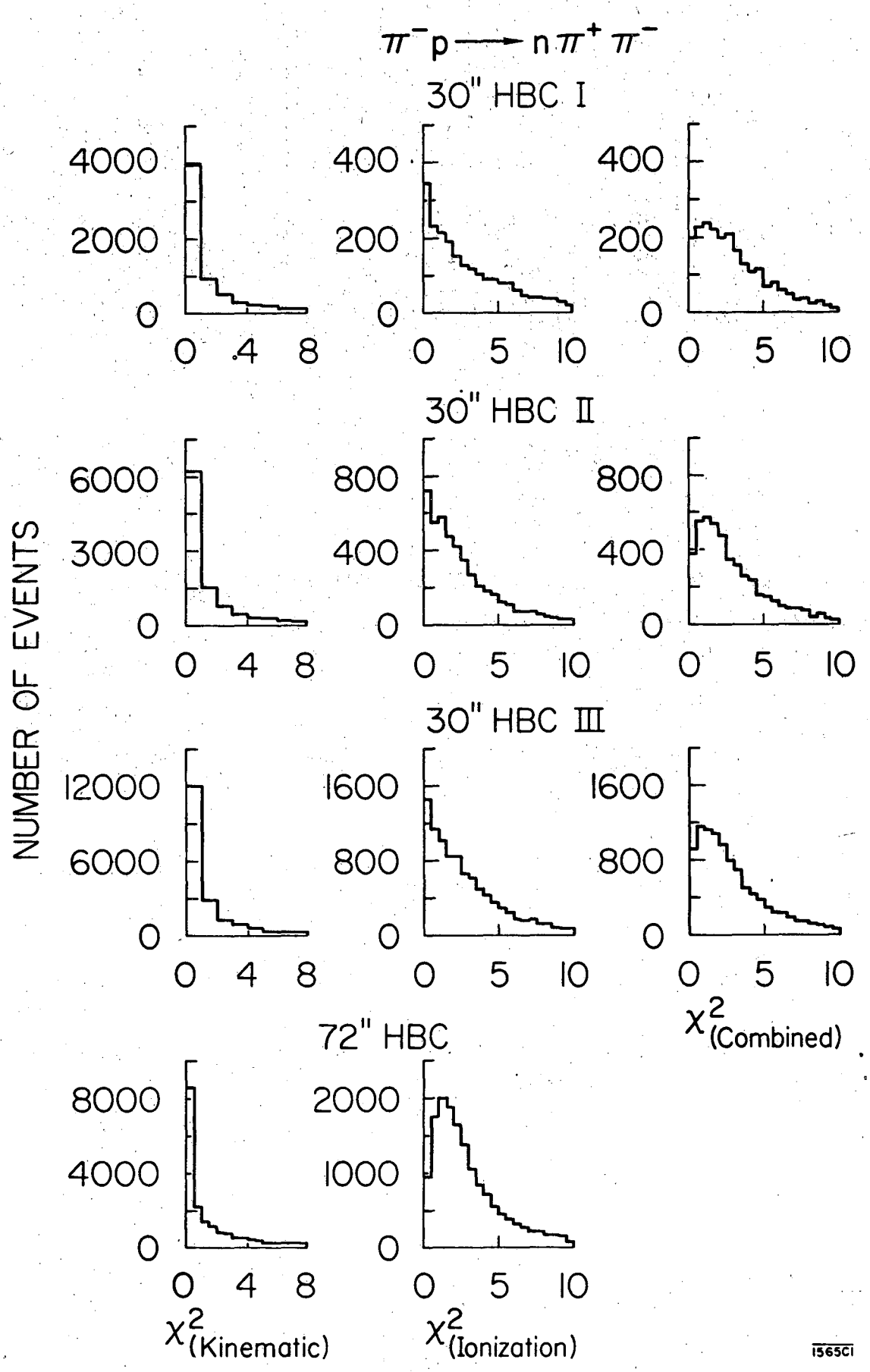
$\pi^- p \longrightarrow n \pi^+ \pi^-$
30" HBC I
30" HBC II
30" HBC III
72" HBC
NUMBER OF EVENTS
$\chi^2_{(Kinematic)}$
$\chi^2_{(Ionization)}$
$\chi^2_{(Combined)}$
1565C1

Fig. 3

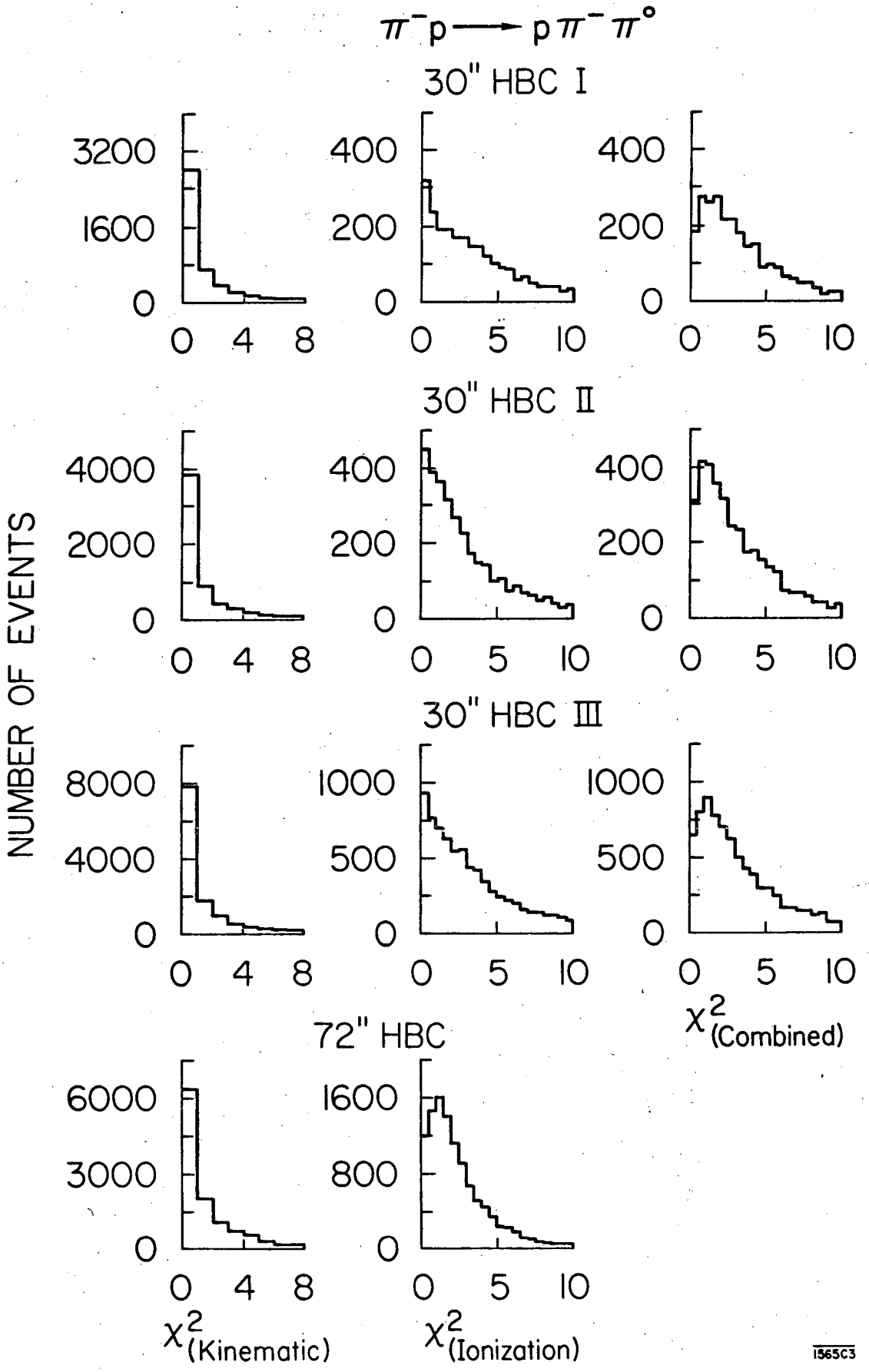
$\pi^- p \longrightarrow p \pi^- \pi^0$
30" HBC I
30" HBC II
30" HBC III
72" HBC
NUMBER OF EVENTS
3200
1600
0
400
200
4000
2000
8000
4000
1000
500
6000
3000
1600
800
0 4 8
0 5 10
$\chi^2_{(Kinematic)}$
$\chi^2_{(Ionization)}$
$\chi^2_{(Combined)}$
1565C3

Fig. 4

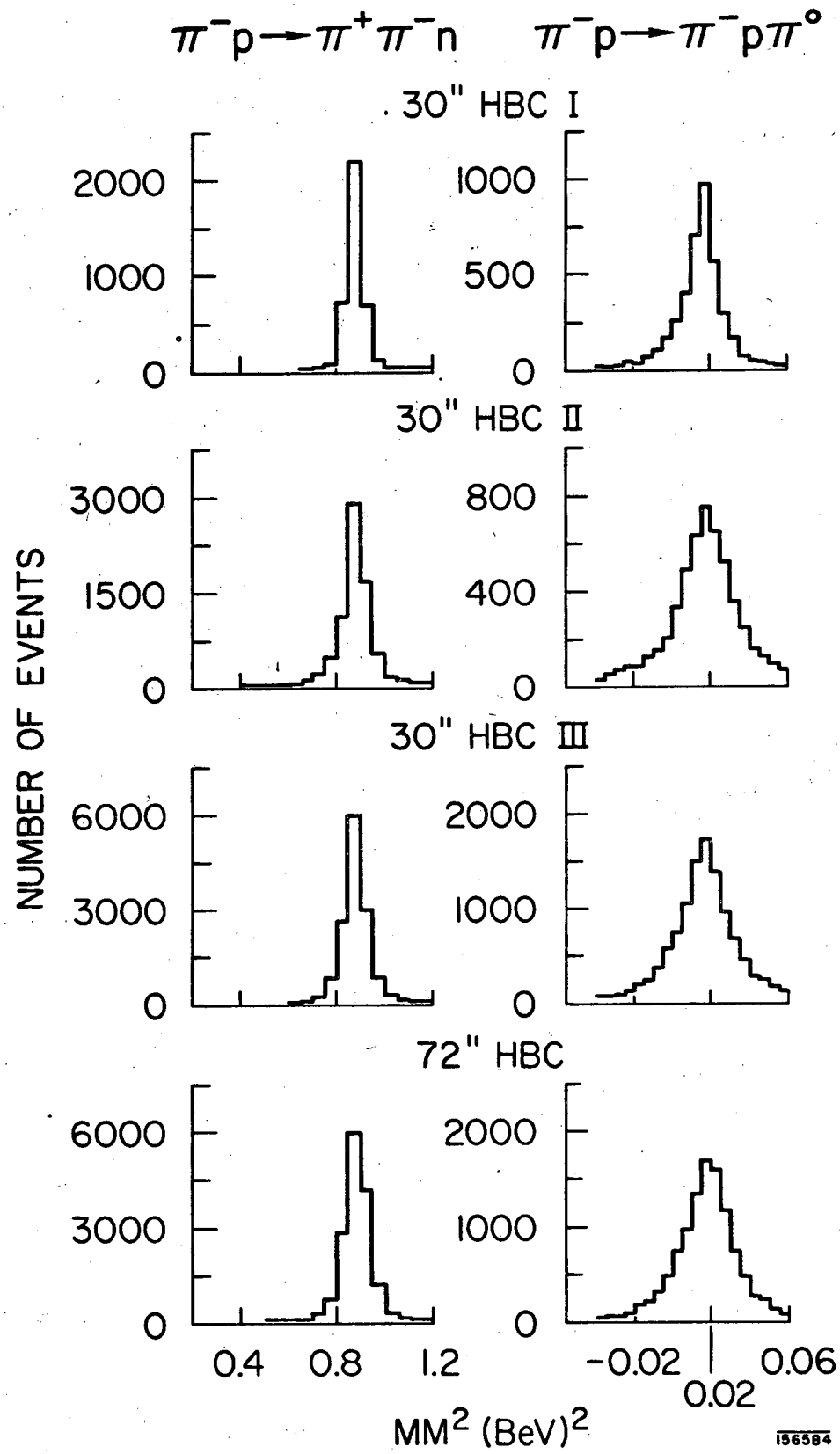
$\pi^- p \rightarrow \pi^+ \pi^- n$
$\pi^- p \rightarrow \pi^- p \pi^0$
30" HBC I
30" HBC II
30" HBC III
72" HBC
NUMBER OF EVENTS
2000
1000
0
1000
500
0
3000
1500
0
800
400
0
6000
3000
0
2000
1000
0
6000
3000
0
2000
1000
0
0.4
0.8
1.2
-0.02
0.02
0.06
$MM^2$ (BeV)$^2$
156584

Fig. 5

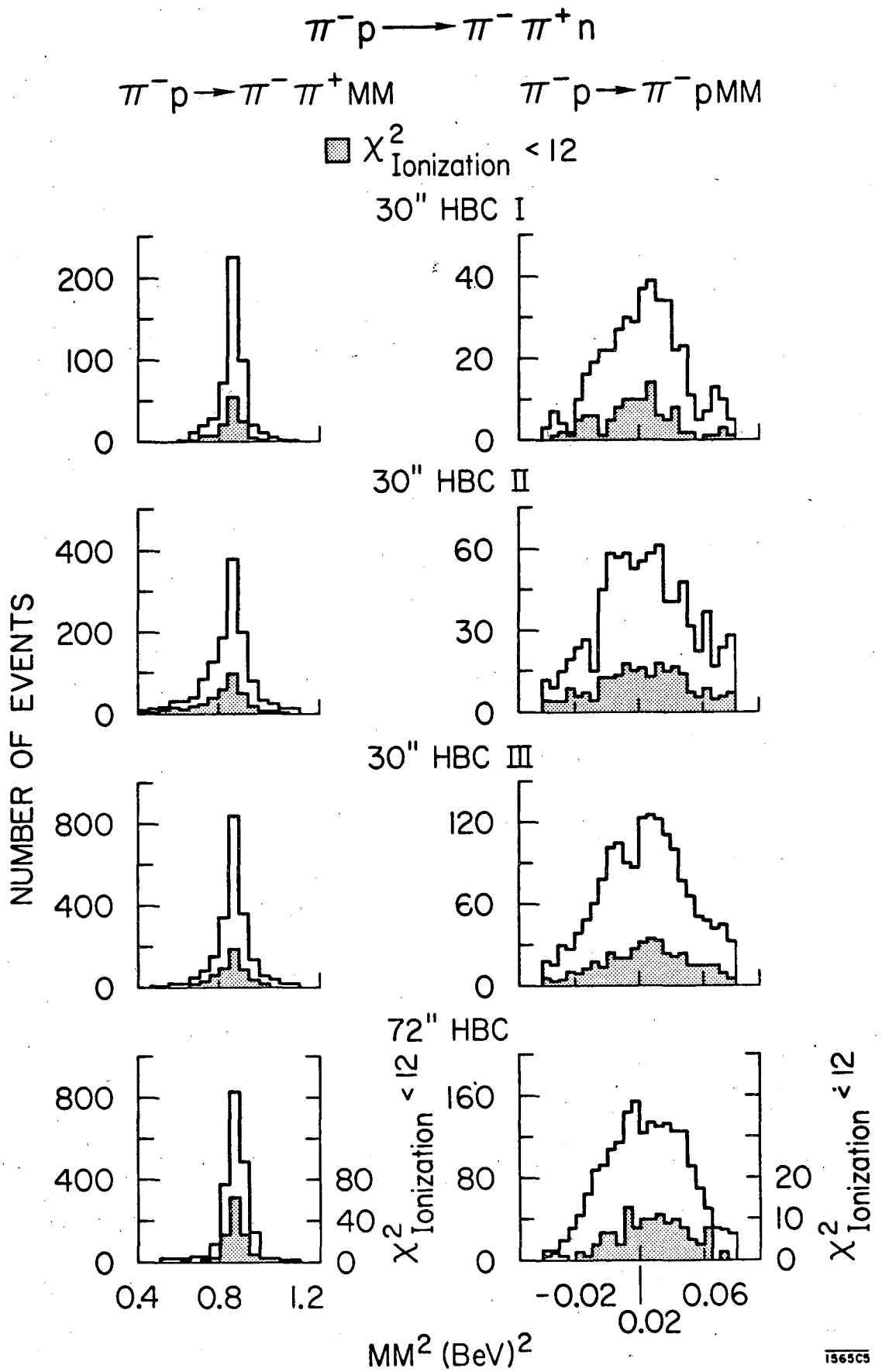
$\pi^- p \longrightarrow \pi^- \pi^+ n$
$\pi^- p \rightarrow \pi^- \pi^+ MM$
$\pi^- p \rightarrow \pi^- p MM$
$\chi^2_{Ionization} < 12$
30" HBC I
30" HBC II
30" HBC III
72" HBC
NUMBER OF EVENTS
$\chi^2_{Ionization} < 12$
$MM^2$ (BeV)$^2$
1565C5

Fig. 6

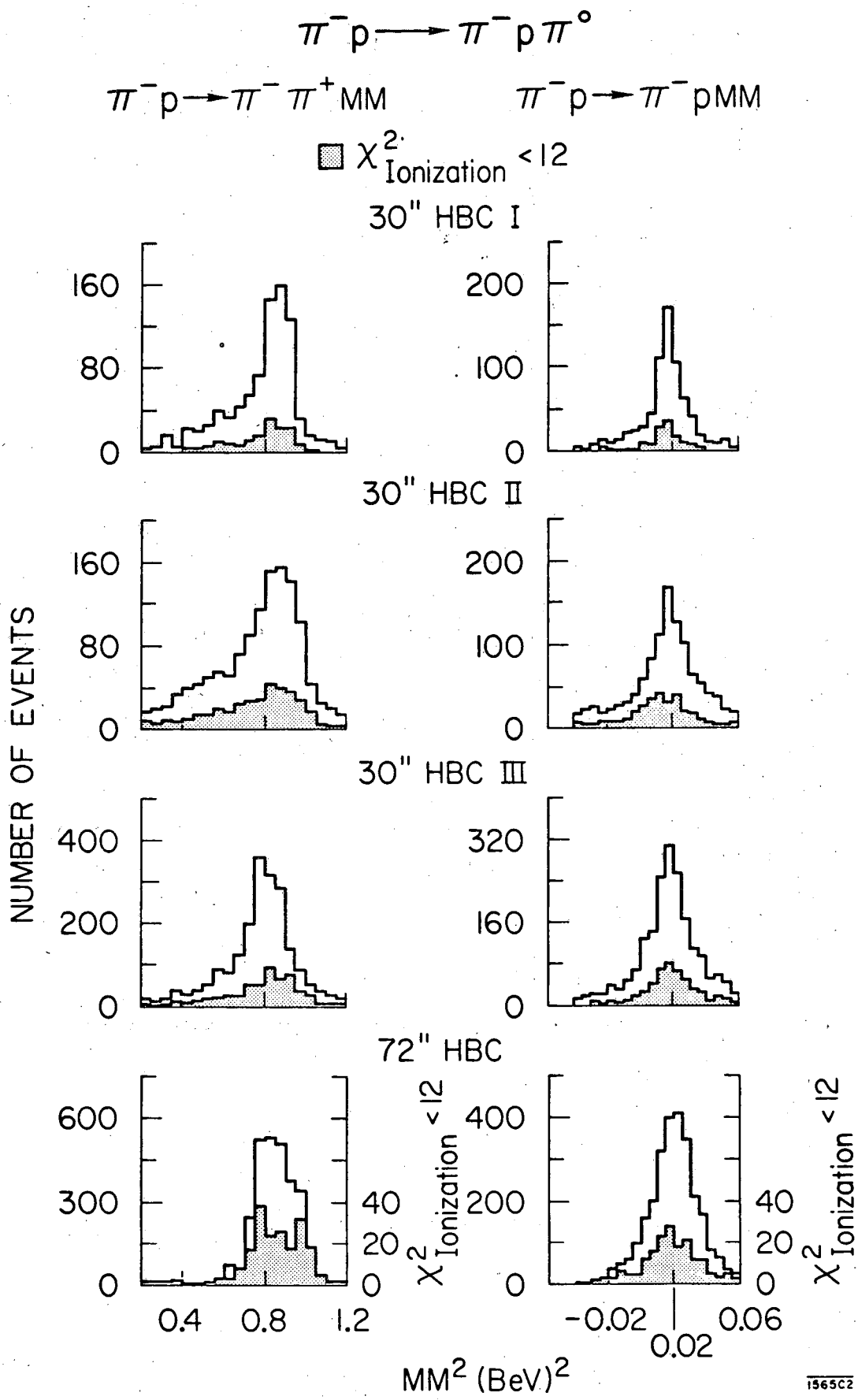
$\pi^- p \longrightarrow \pi^- p \pi^0$
$\pi^- p \rightarrow \pi^- \pi^+ MM$
$\pi^- p \rightarrow \pi^- p MM$
$\chi^2_{Ionization} < 12$
30" HBC I
30" HBC II
30" HBC III
72" HBC
NUMBER OF EVENTS
$\chi^2_{Ionization} < 12$
0.4
0.8
1.2
-0.02
0.02
0.06
$MM^2$ (BeV)$^2$
1565C2

Fig. 7

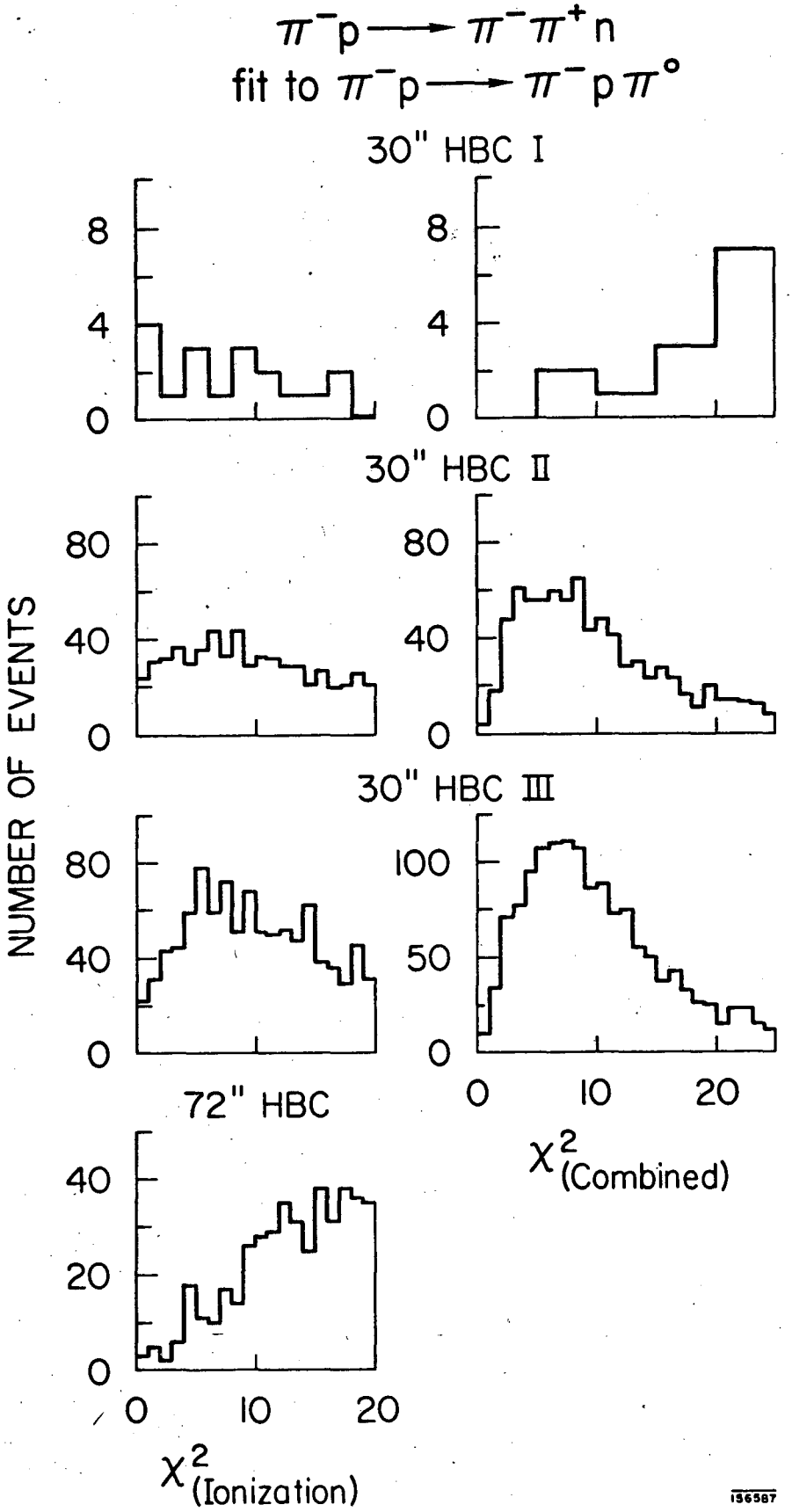
$\pi^- p \longrightarrow \pi^- \pi^+ n$
fit to $\pi^- p \longrightarrow \pi^- p \pi^0$
30" HBC I
30" HBC II
30" HBC III
72" HBC
NUMBER OF EVENTS
$\chi^2_{(Combined)}$
$\chi^2_{(Ionization)}$
156587

Fig. 8

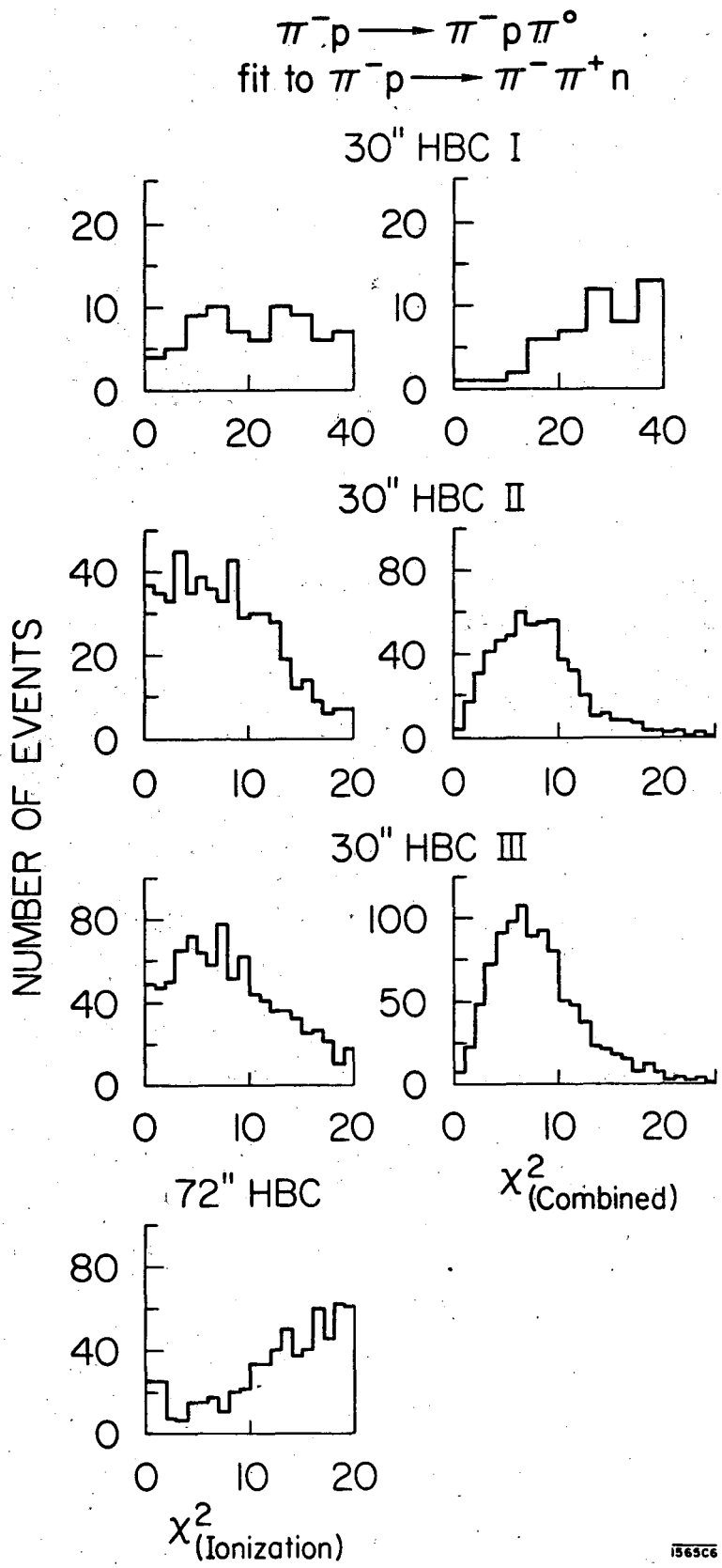
$\pi^- p \longrightarrow \pi^- p \pi^0$
fit to $\pi^- p \longrightarrow \pi^- \pi^+ n$
30" HBC I
30" HBC II
30" HBC III
72" HBC
NUMBER OF EVENTS
$\chi^2_{(Combined)}$
$\chi^2_{(Ionization)}$
1565C6

Fig. 9

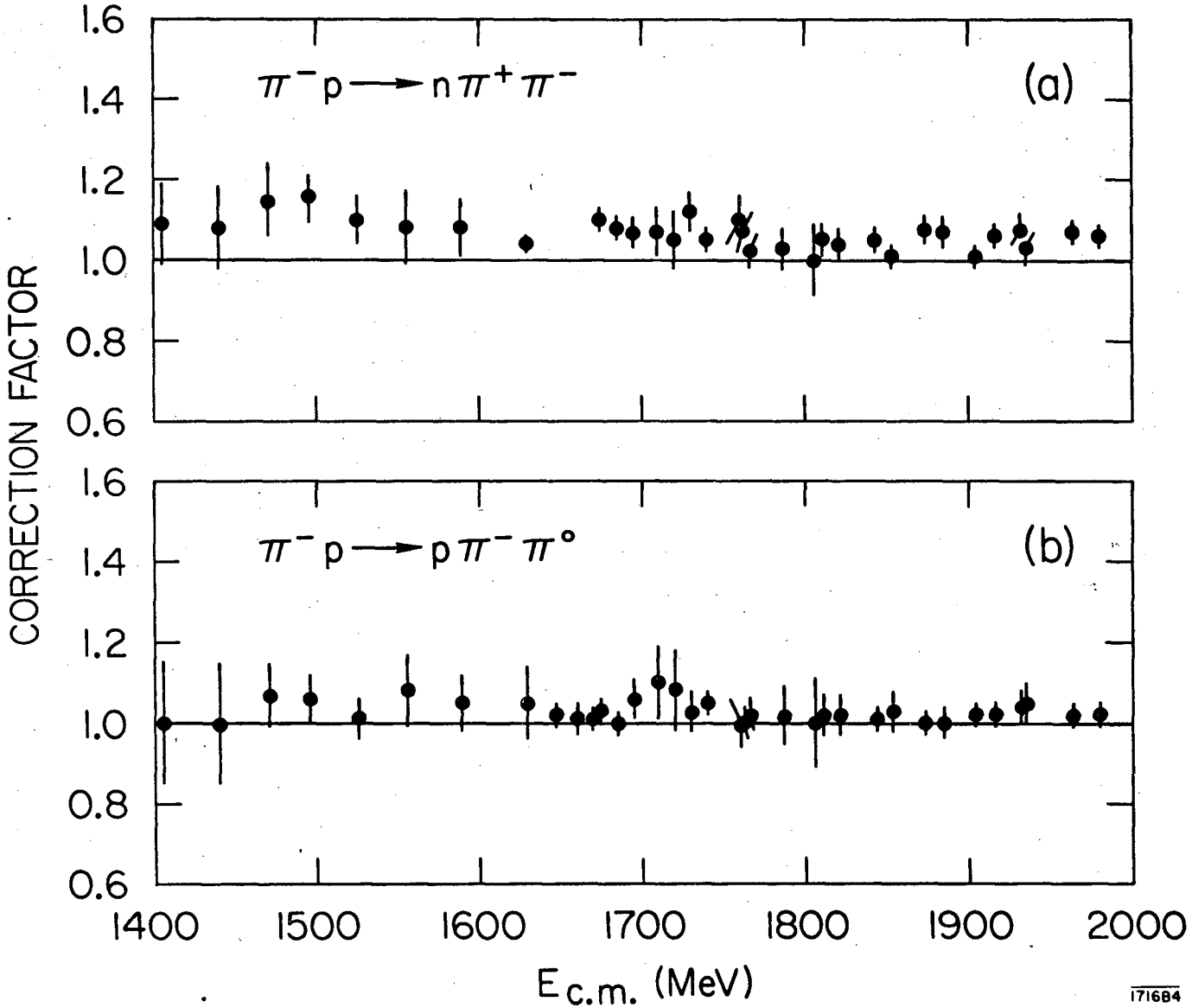
1.6
1.4
1.2
1.0
0.8
0.6
$\pi^- p \rightarrow n \pi^+ \pi^-$
(a)
CORRECTION FACTOR
$\pi^- p \rightarrow p \pi^- \pi^\circ$
(b)
1400
1500
1600
1700
1800
1900
2000
$E_{c.m.}$ (MeV)
171684

Fig. 10

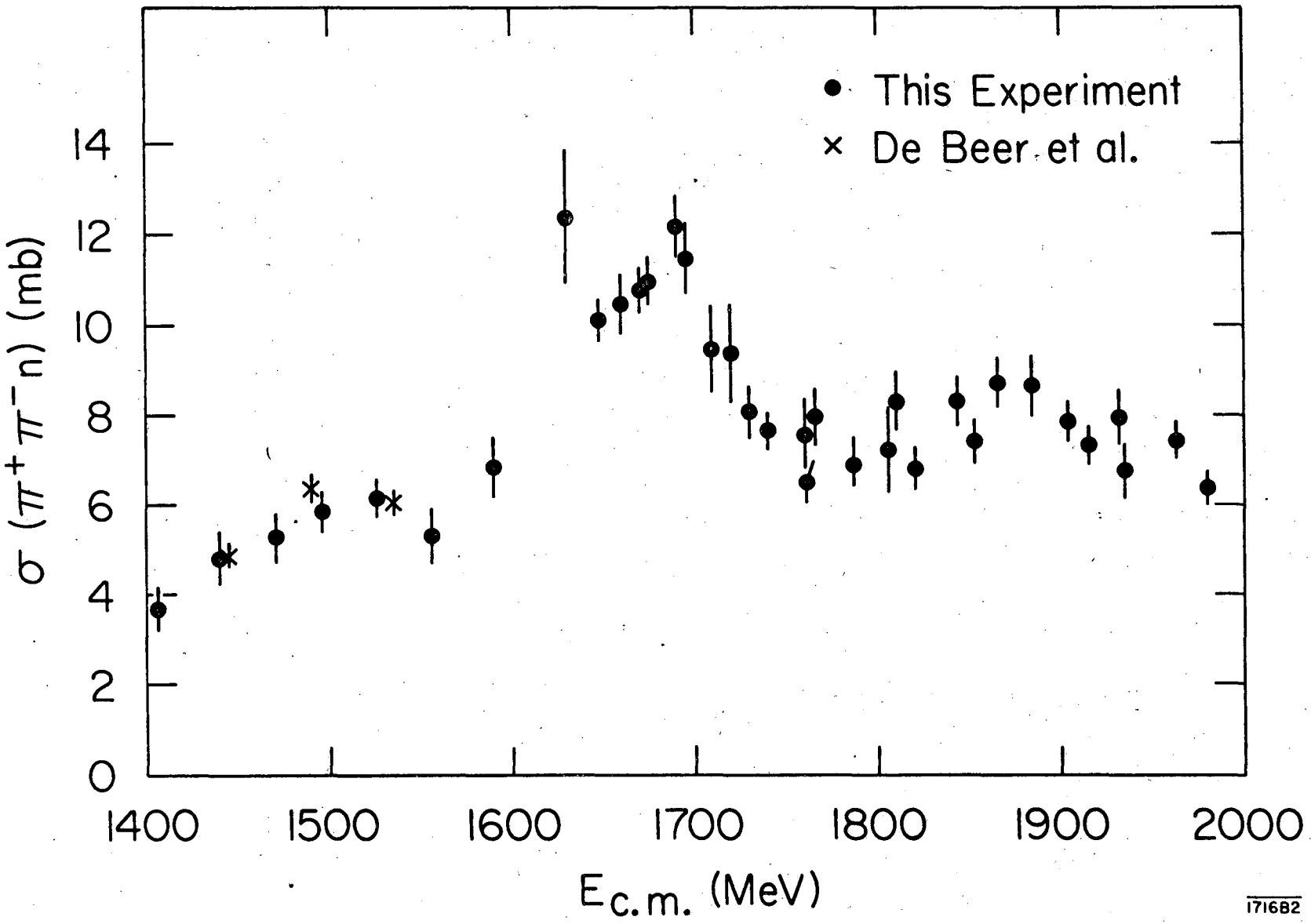
This Experiment
De Beer et al.
σ (π⁺π⁻n) (mb)
0
2
4
6
8
10
12
14
1400
1500
1600
1700
1800
1900
2000
E c.m. (MeV)
171682

Fig. 11

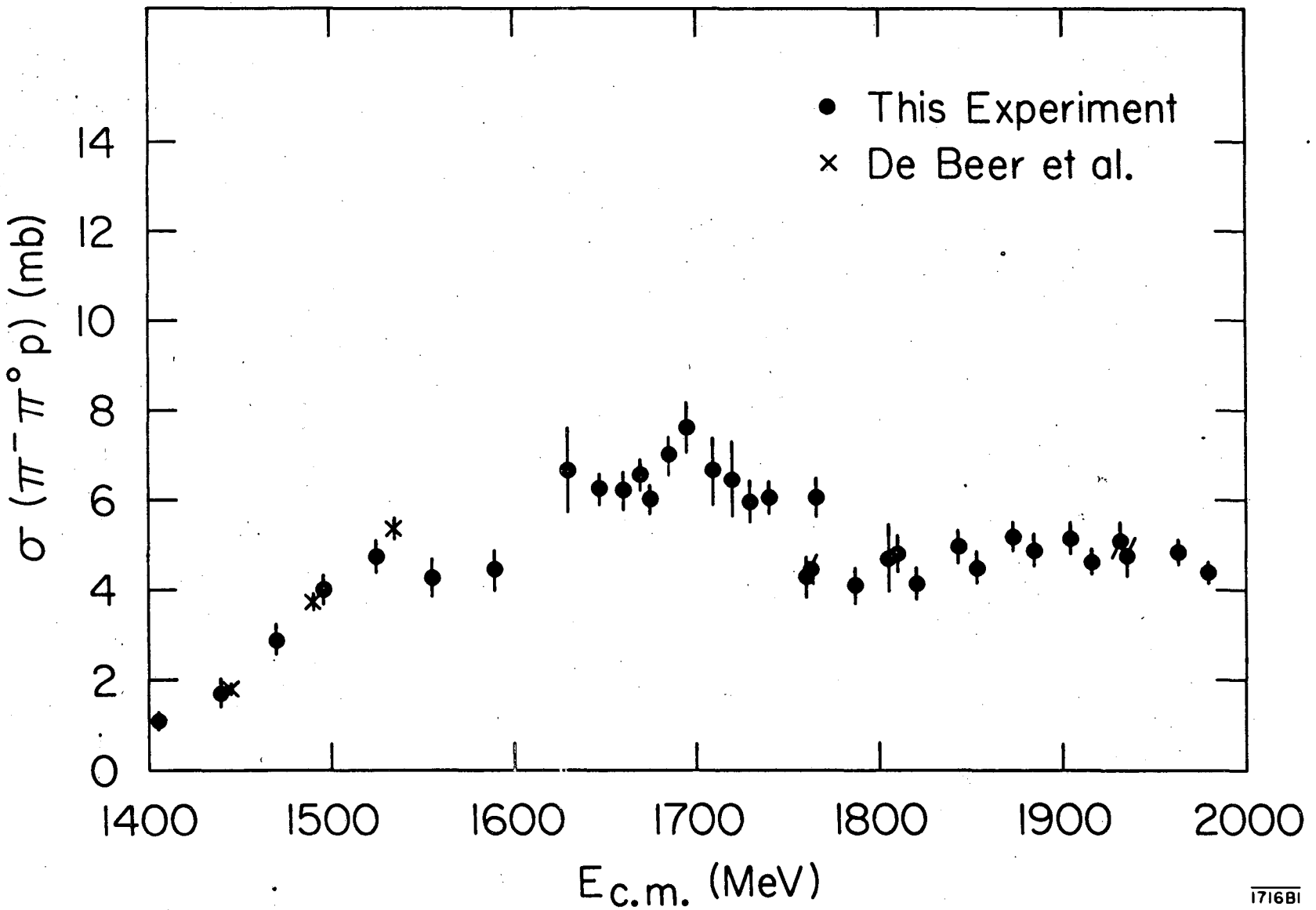
This Experiment
De Beer et al.
σ (π⁻π°p) (mb)
0
2
4
6
8
10
12
14
1400
1500
1600
1700
1800
1900
2000
E c.m. (MeV)
1716B1

Fig. 12

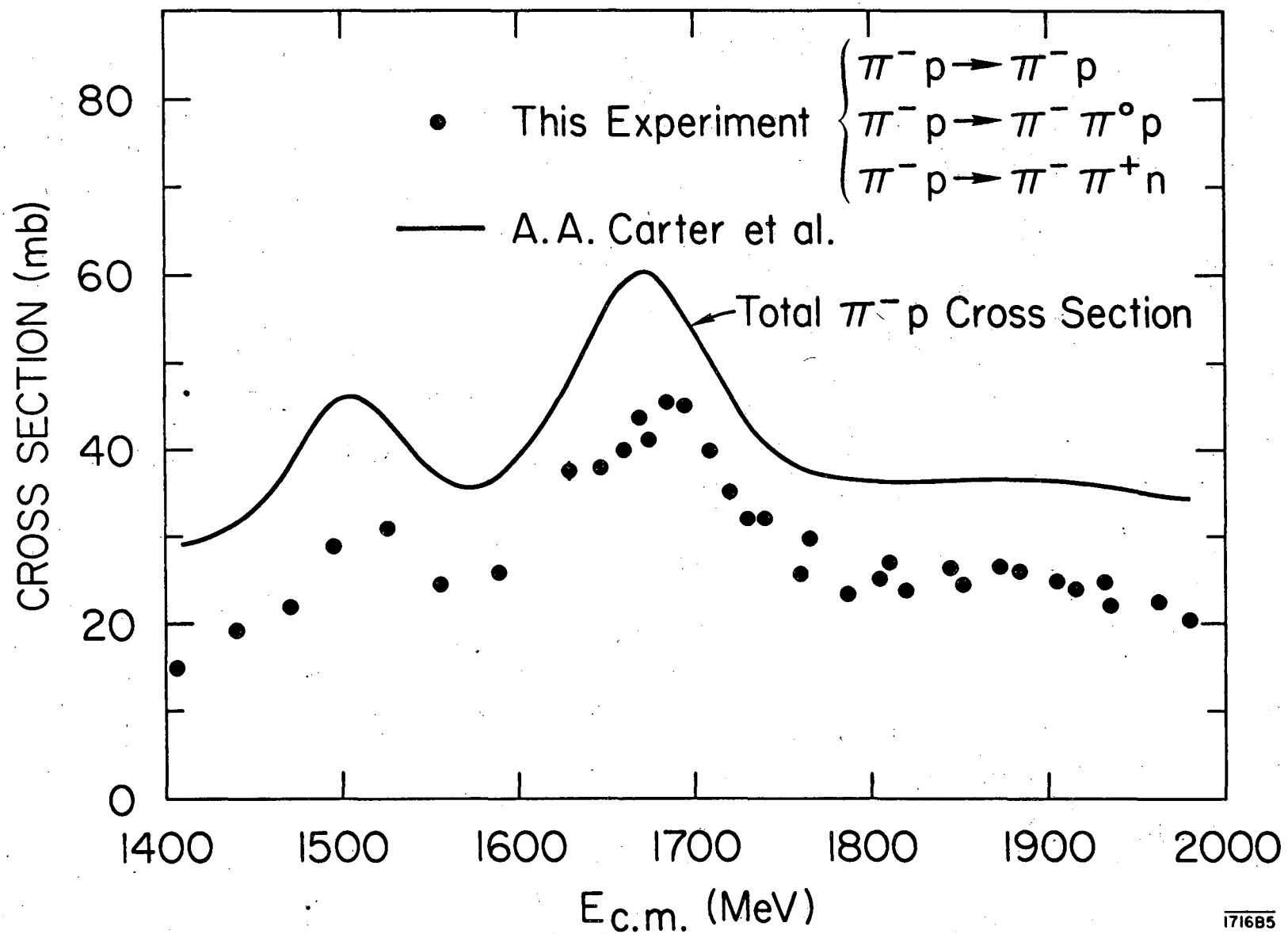
This Experiment
$\pi^- p \rightarrow \pi^- p$
$\pi^- p \rightarrow \pi^- \pi^0 p$
$\pi^- p \rightarrow \pi^- \pi^+ n$
A. A. Carter et al.
Total $\pi^- p$ Cross Section
CROSS SECTION (mb)
0
20
40
60
80
1400
1500
1600
1700
1800
1900
2000
$E_{c.m.}$ (MeV)
1716B5

Fig. 13

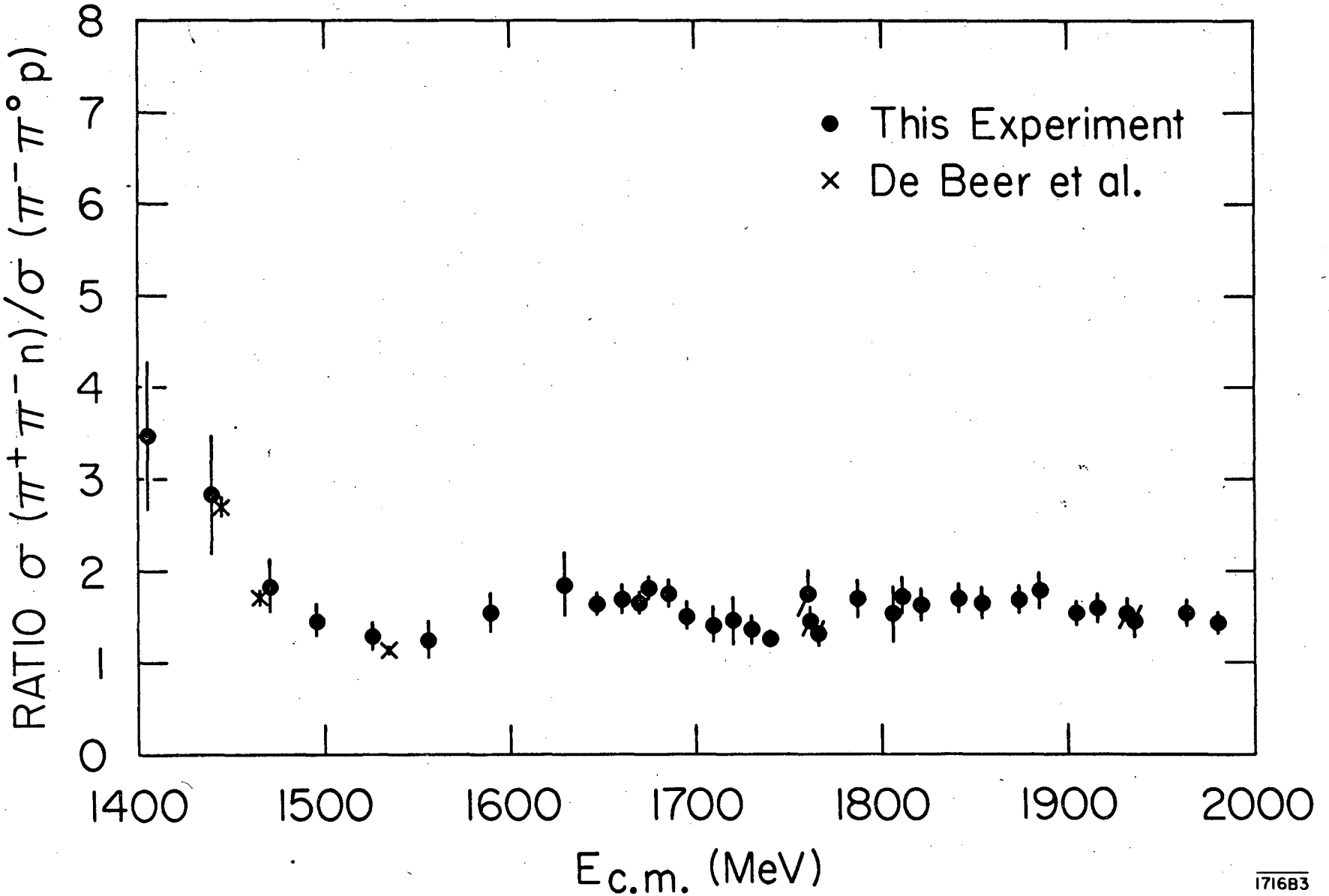
RATIO σ (π⁺π⁻n)/σ (π⁻π°p)
0
1
2
3
4
5
6
7
8
1400
1500
1600
1700
1800
1900
2000
E c.m. (MeV)
This Experiment
De Beer et al.
1716B3

Fig. 14

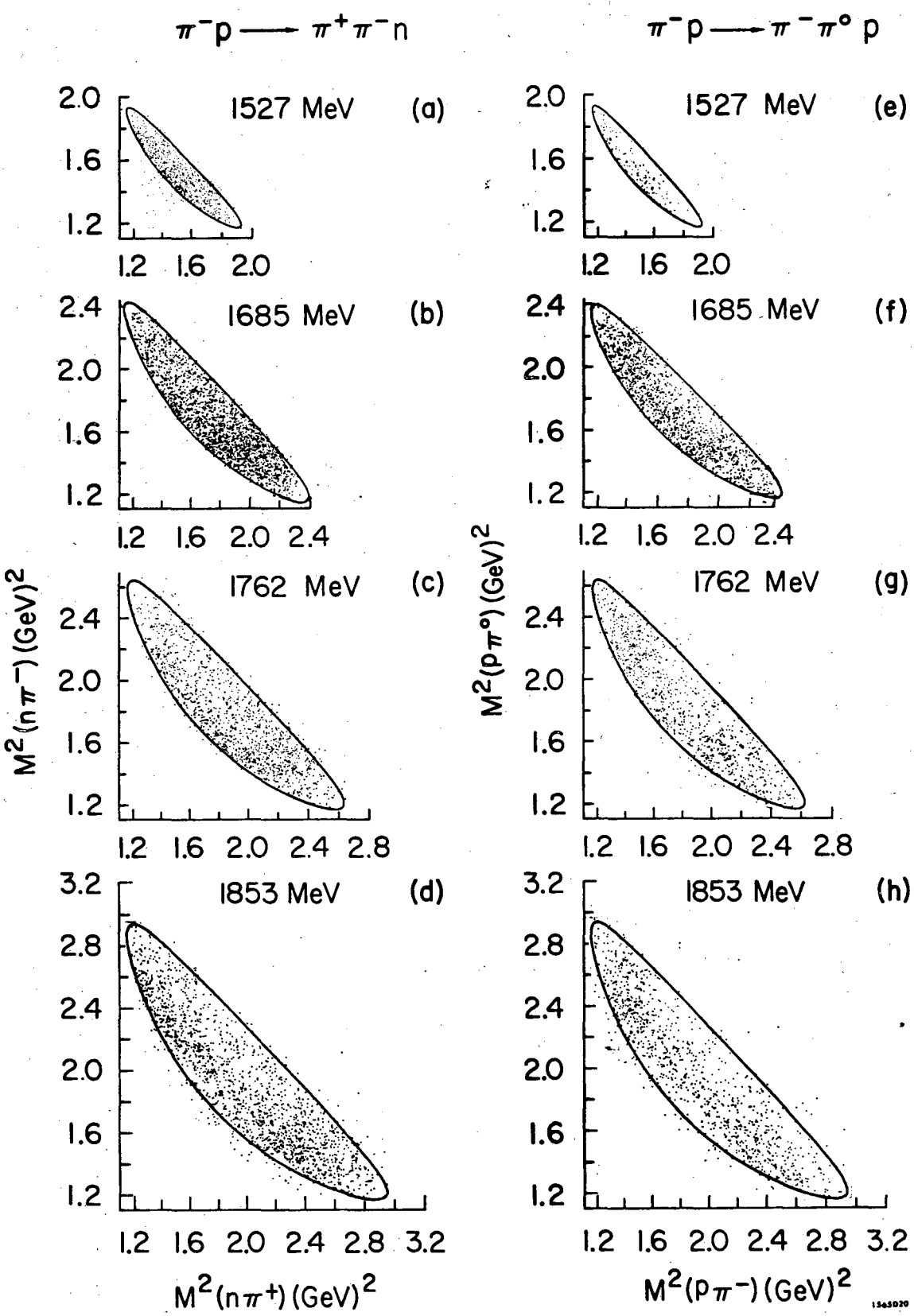
$\pi^- p \longrightarrow \pi^+ \pi^- n$
$\pi^- p \longrightarrow \pi^- \pi^0 p$
1527 MeV (a)
1685 MeV (b)
1762 MeV (c)
1853 MeV (d)
1527 MeV (e)
1685 MeV (f)
1762 MeV (g)
1853 MeV (h)
$M^2(n\pi^-)$ (GeV)$^2$
$M^2(p\pi^0)$ (GeV)$^2$
$M^2(n\pi^+)$ (GeV)$^2$
$M^2(p\pi^-)$ (GeV)$^2$

Fig. 15

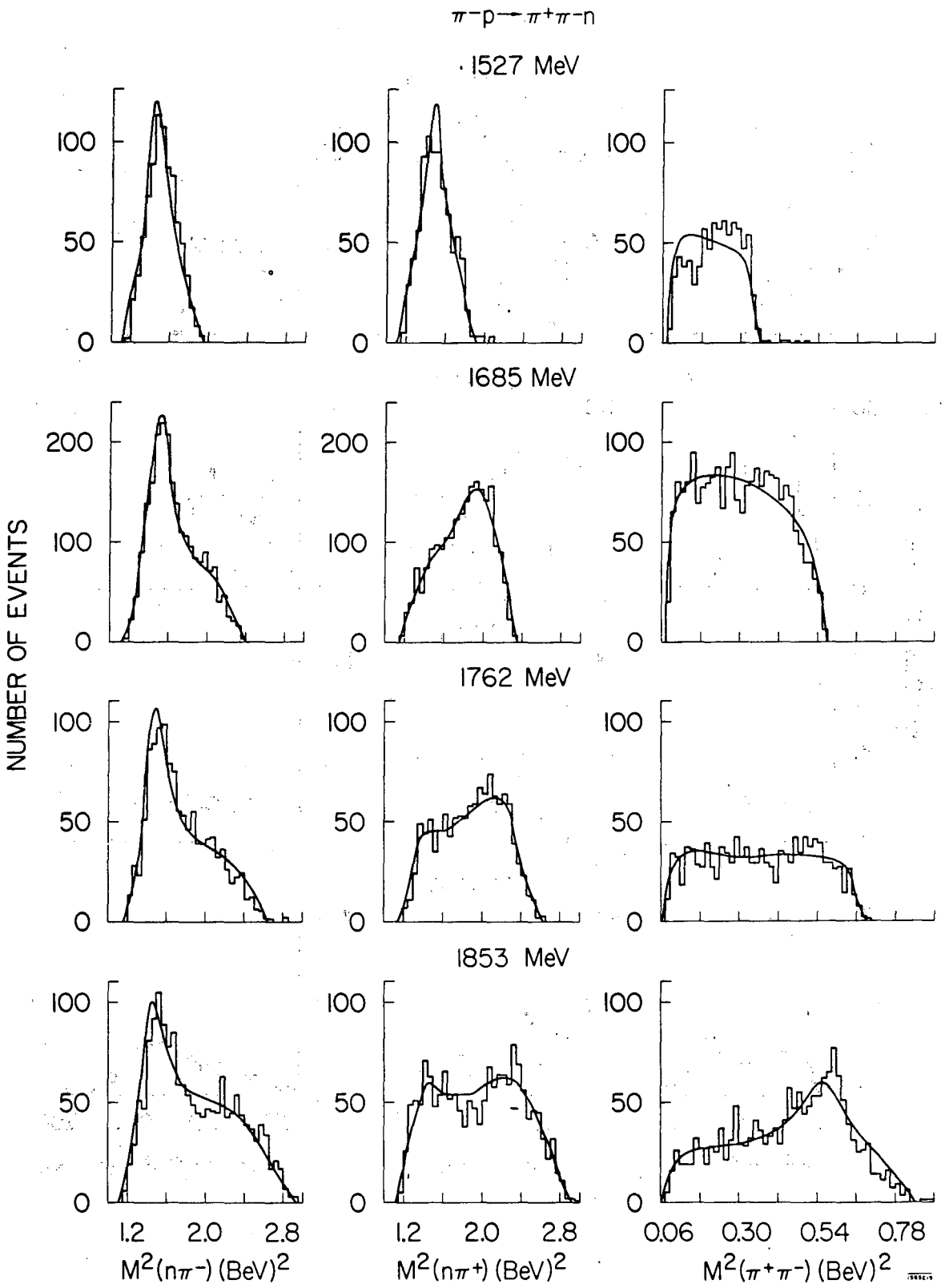
π⁻p→π⁺π⁻n
1527 MeV
1685 MeV
1762 MeV
1853 MeV
NUMBER OF EVENTS
M²(nπ⁻) (BeV)²
M²(nπ⁺) (BeV)²
M²(π⁺π⁻) (BeV)²

Fig. 16

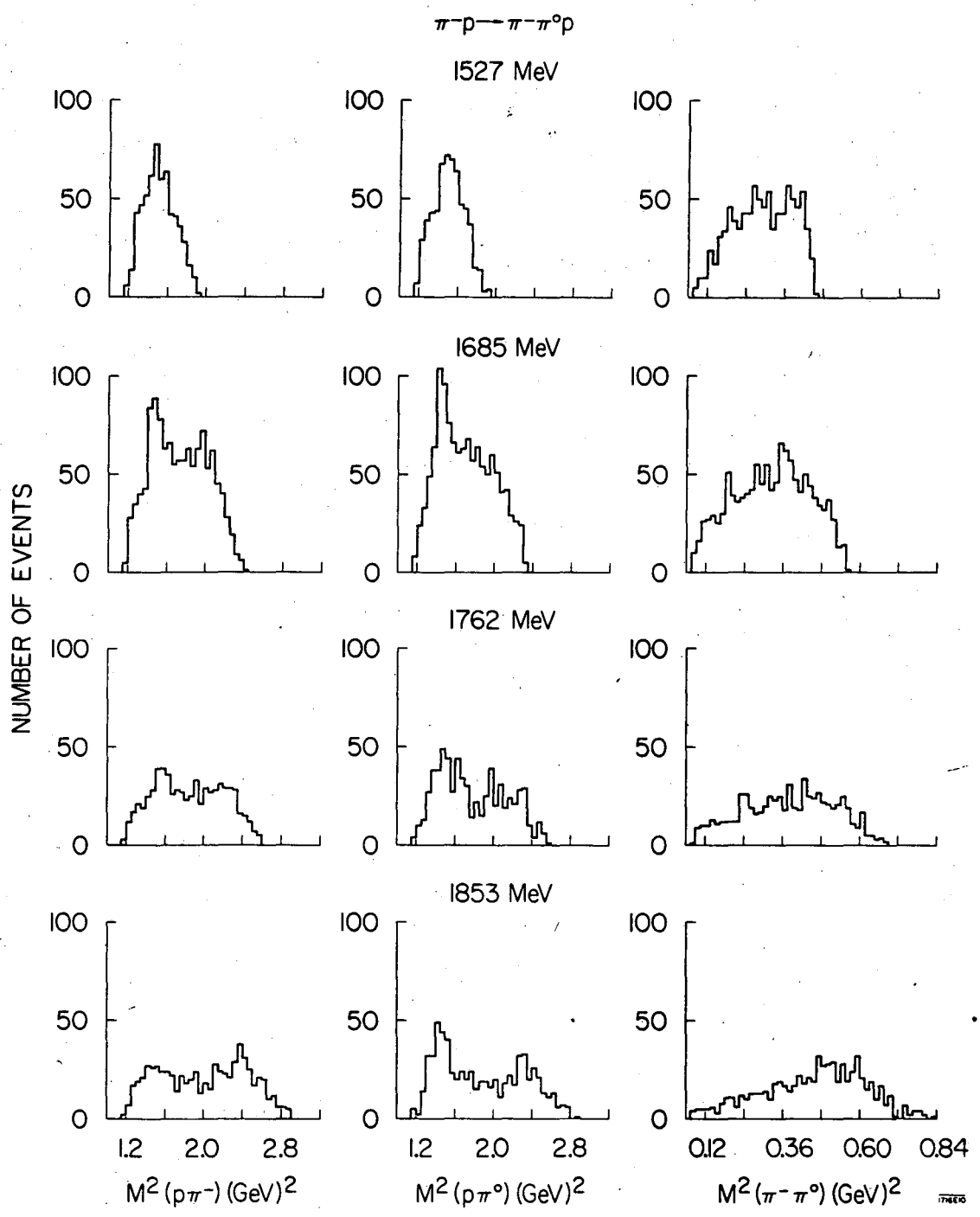
π⁻p → π⁻π°p
1527 MeV
1685 MeV
1762 MeV
1853 MeV
NUMBER OF EVENTS
100
50
0
1.2
2.0
2.8
0.12
0.36
0.60
0.84
M² (pπ⁻) (GeV)²
M² (pπ°) (GeV)²
M² (π⁻π°) (GeV)²

Fig. 17

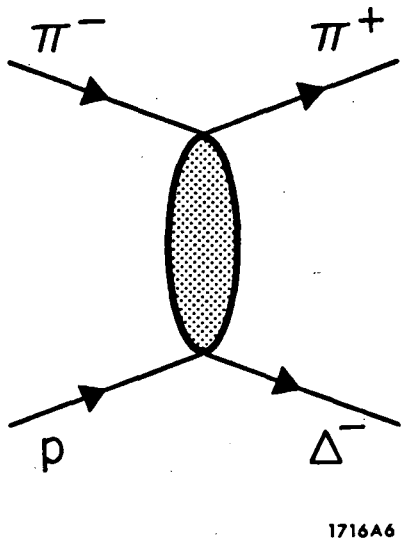


Fig. 18

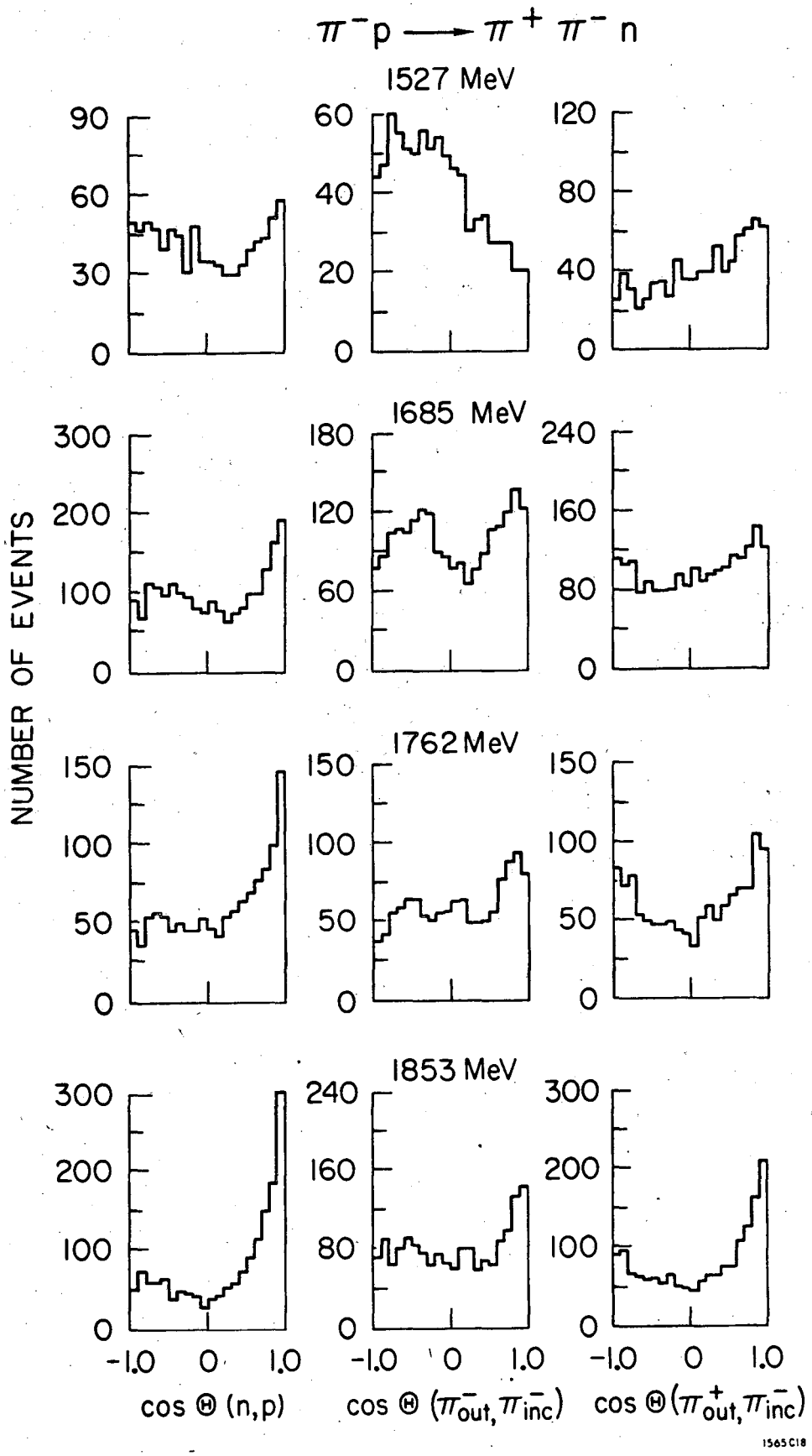
$\pi^- p \longrightarrow \pi^+ \pi^- n$
1527 MeV
1685 MeV
1762 MeV
1853 MeV
NUMBER OF EVENTS
cos Θ (n,p)
cos Θ ($\pi^-_{out}, \pi^-_{inc}$)
cos Θ ($\pi^+_{out}, \pi^-_{inc}$)
1565C18

Fig. 19

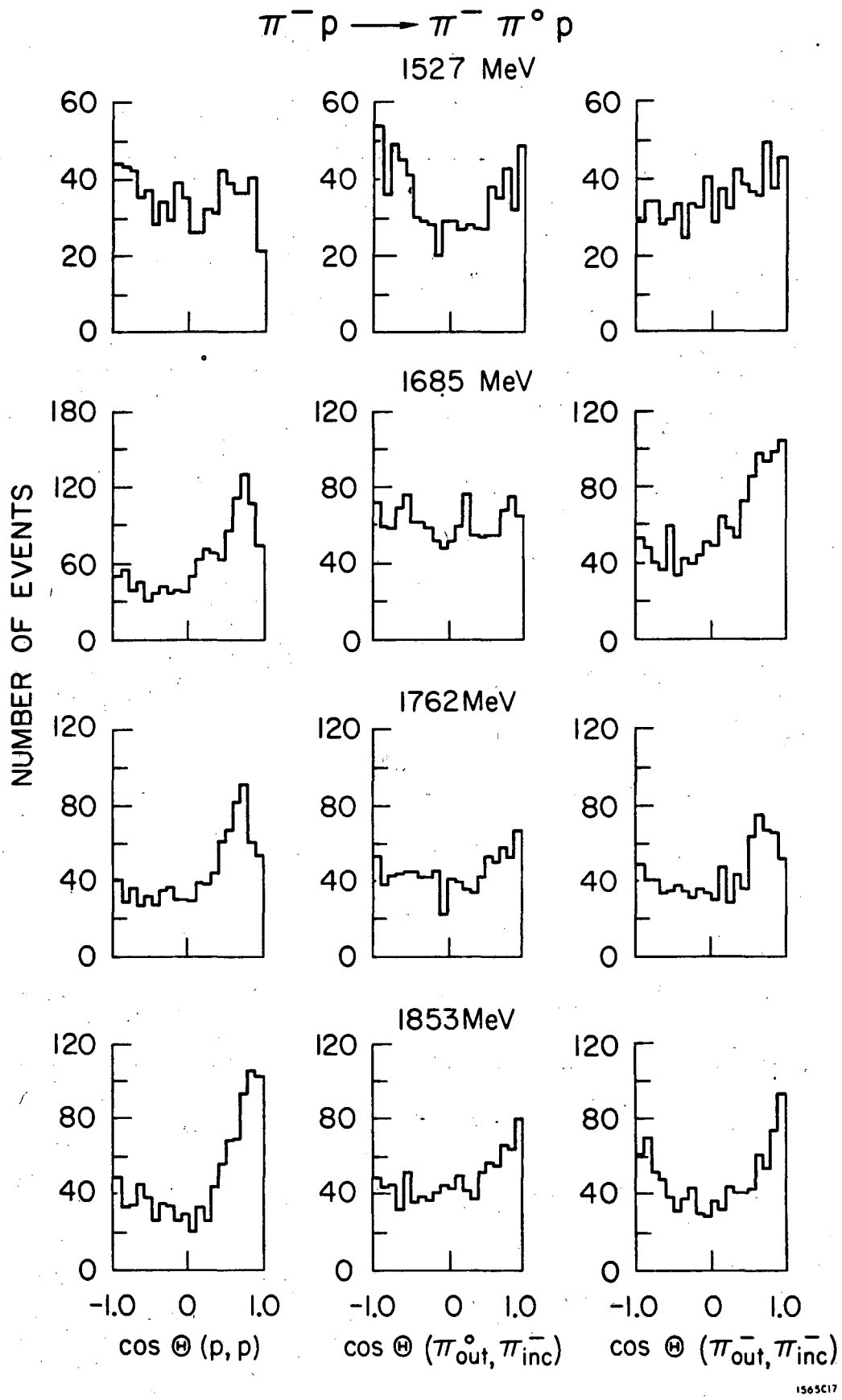
$\pi^- p \longrightarrow \pi^- \pi^\circ p$
1527 MeV
1685 MeV
1762 MeV
1853 MeV
NUMBER OF EVENTS
cos Θ (p, p)
cos Θ ($\pi^\circ_{out}, \pi^-_{inc}$)
cos Θ ($\pi^-_{out}, \pi^-_{inc}$)
1565C17

Fig. 20

MOMENTS IN THE FINAL STATE $\pi^-\pi^+n$

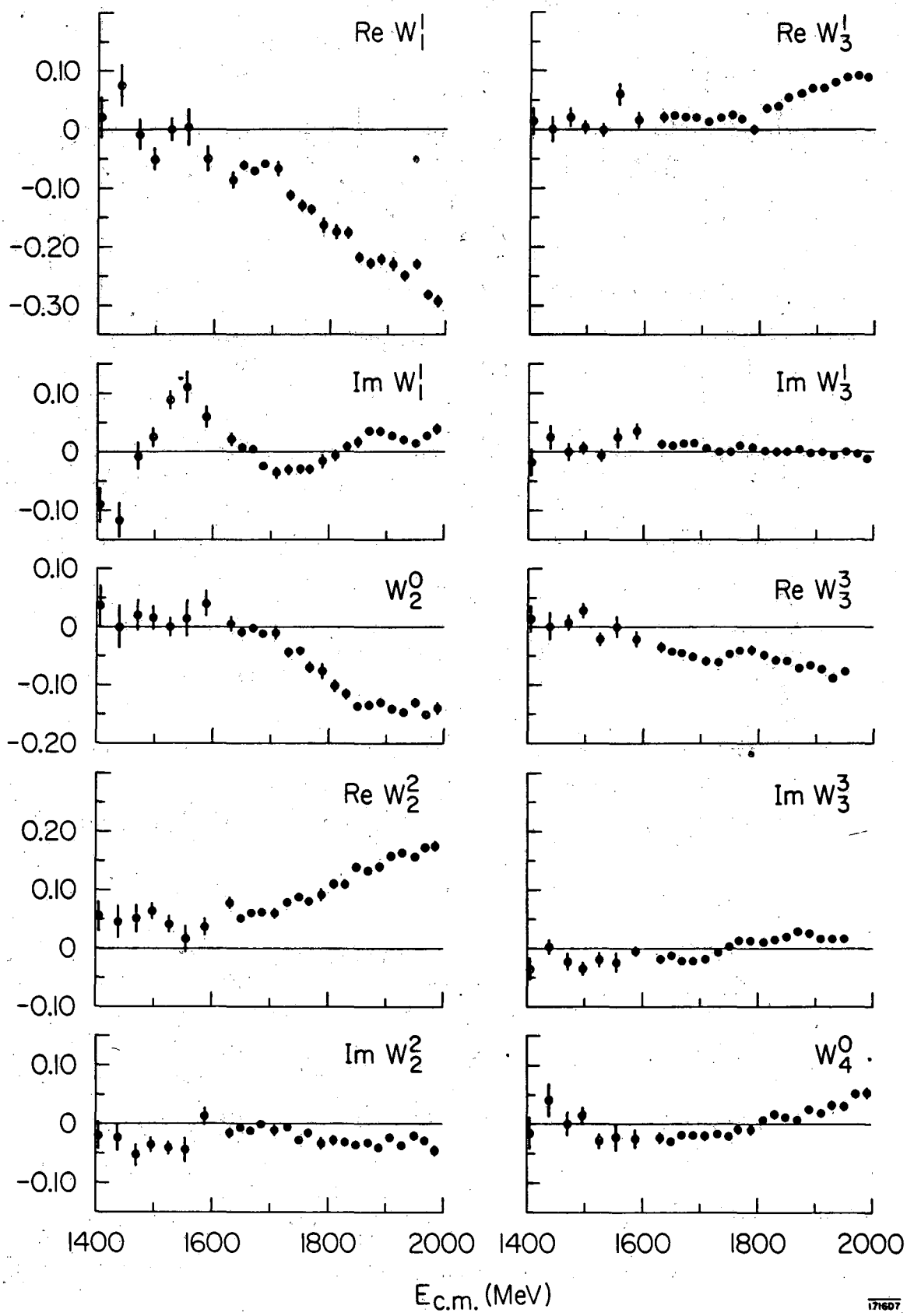


Fig. 21A

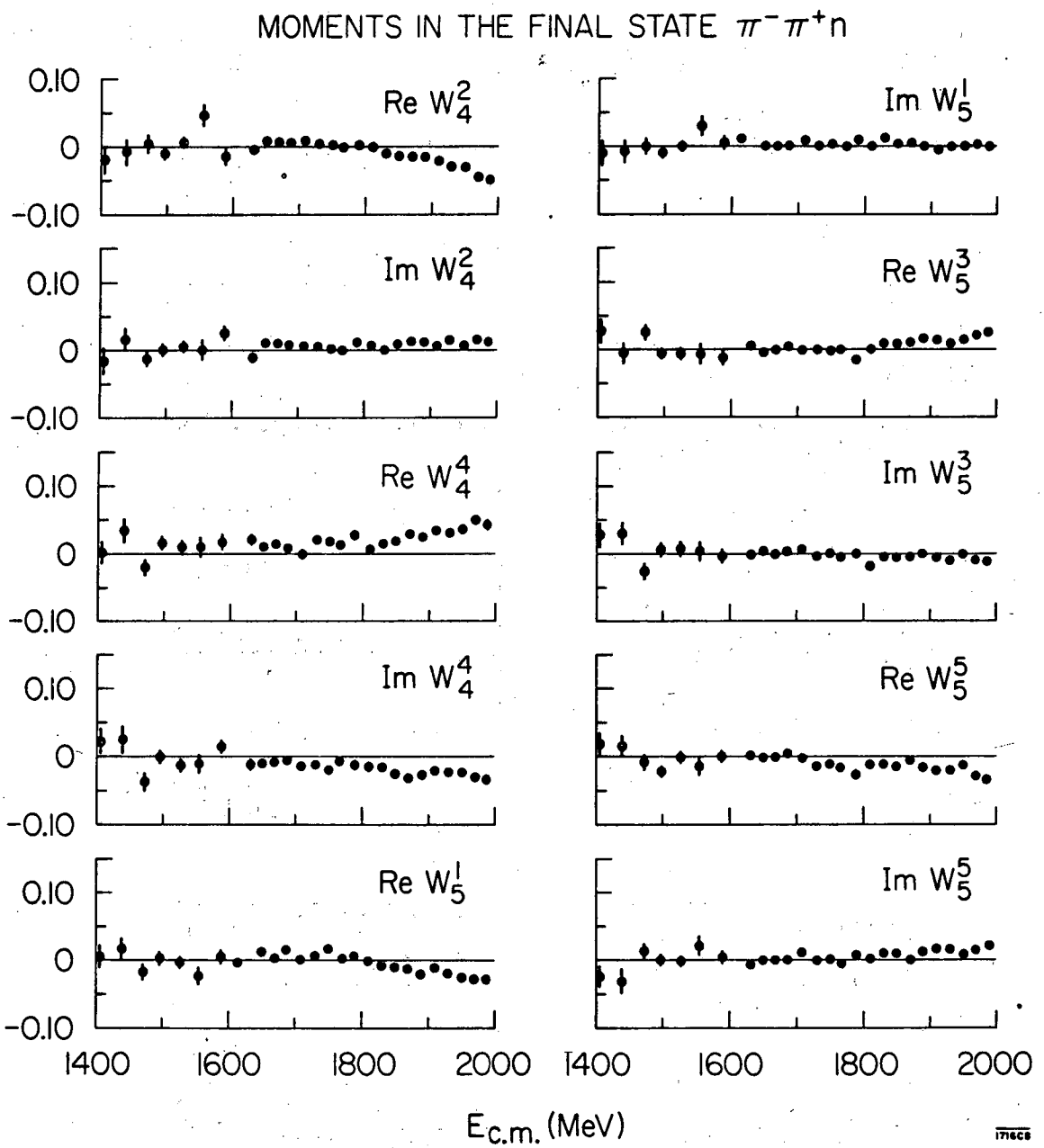
MOMENTS IN THE FINAL STATE $\pi^-\pi^+n$
Re $W_4^2$
Im $W_4^2$
Re $W_4^4$
Im $W_4^4$
Re $W_5^1$
Im $W_5^1$
Re $W_5^3$
Im $W_5^3$
Re $W_5^5$
Im $W_5^5$
0.10
0
-0.10
1400
1600
1800
2000
$E_{c.m.}$ (MeV)

Fig. 21B

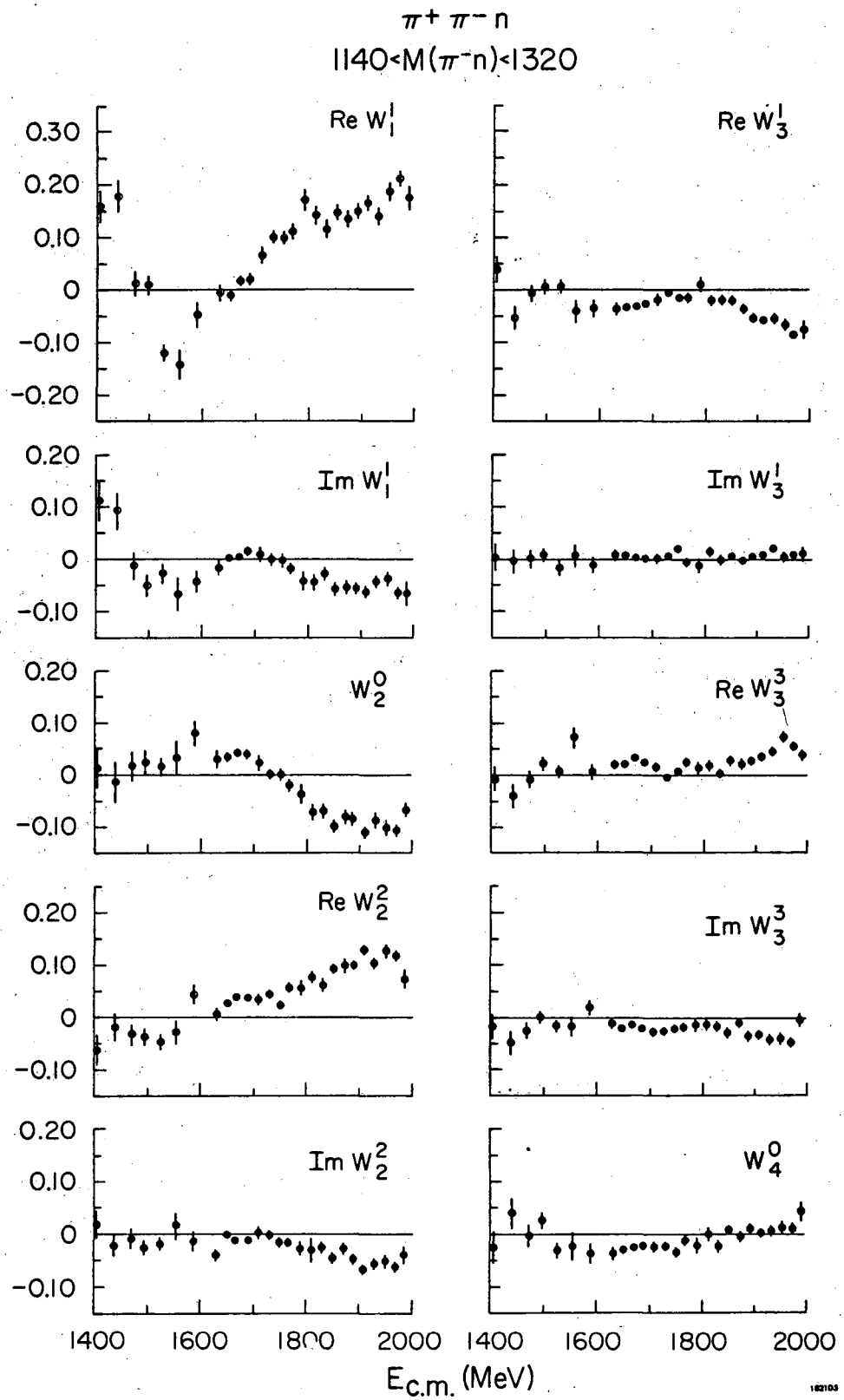
π+ π− n
1140<M(π−n)<1320
Re W¹₁
Re W¹₃
Im W¹₁
Im W¹₃
W⁰₂
Re W³₃
Re W²₂
Im W³₃
Im W²₂
W⁰₄
0.30
0.20
0.10
0
−0.10
−0.20
1400
1600
1800
2000
E c.m. (MeV)

Fig. 22A

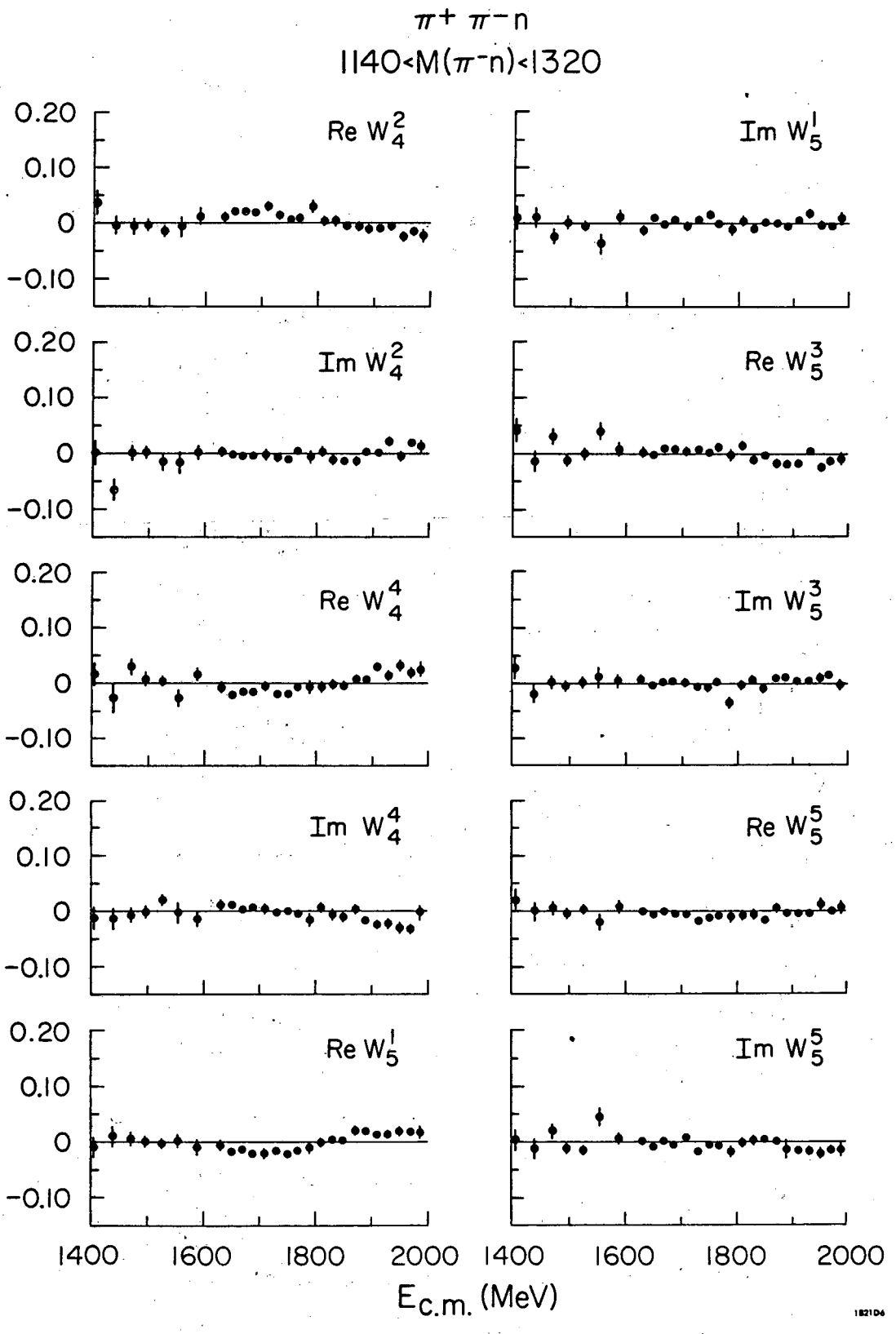
π+ π−n
1140<M(π−n)<1320
Re W$_4^2$
Im W$_5^1$
Im W$_4^2$
Re W$_5^3$
Re W$_4^4$
Im W$_5^3$
Im W$_4^4$
Re W$_5^5$
Re W$_5^1$
Im W$_5^5$
0.20
0.10
0
−0.10
1400
1600
1800
2000
E$_{c.m.}$ (MeV)
1821D6

Fig. 22B

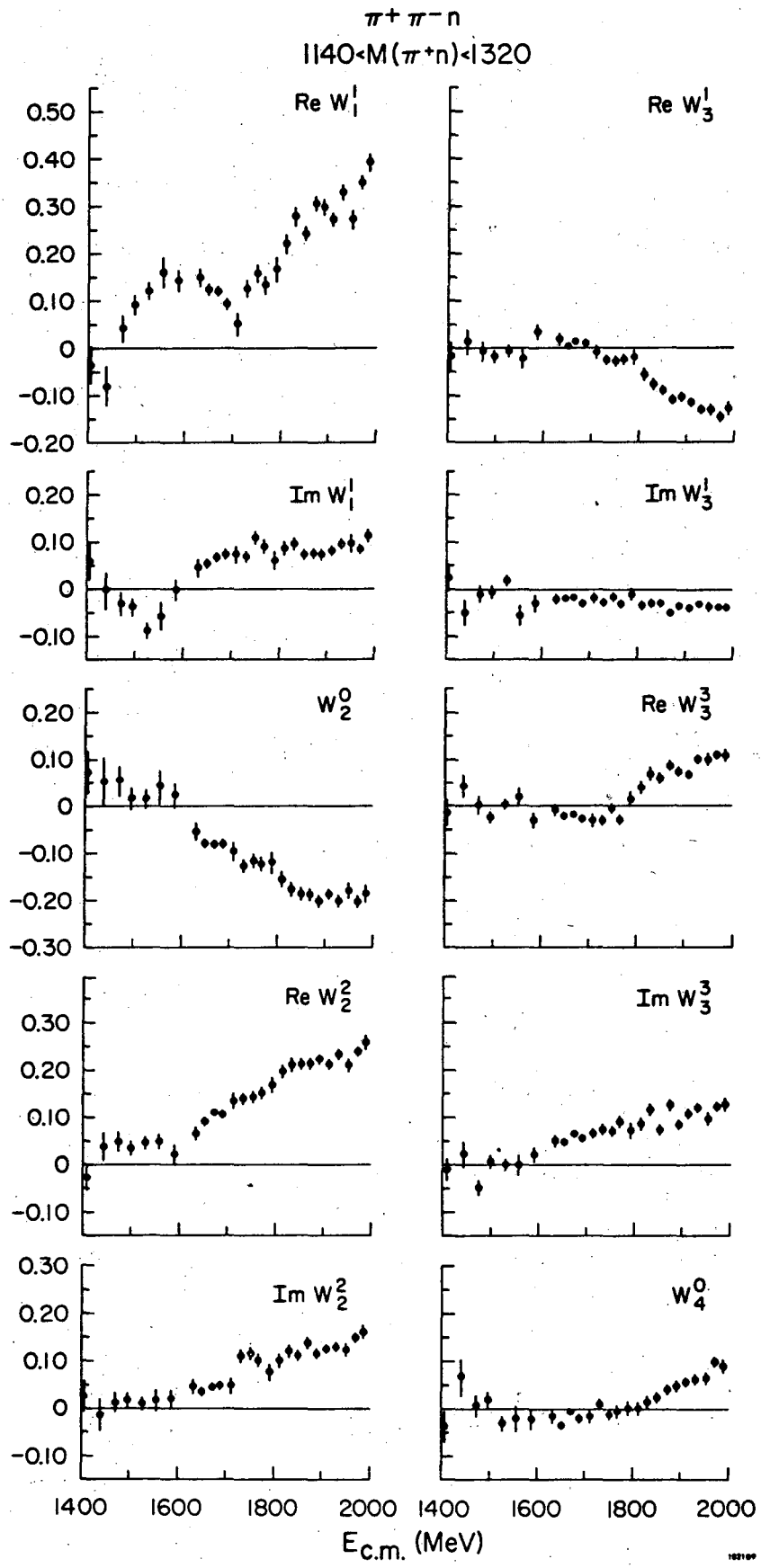
$\pi^+\pi^-n$
1140<M($\pi^+$n)<1320
Re $W_1^1$
Re $W_3^1$
Im $W_1^1$
Im $W_3^1$
$W_2^0$
Re $W_3^3$
Re $W_2^2$
Im $W_3^3$
Im $W_2^2$
$W_4^0$
0.50
0.40
0.30
0.20
0.10
0
-0.10
-0.20
-0.30
1400
1600
1800
2000
$E_{c.m.}$ (MeV)

Fig. 23A

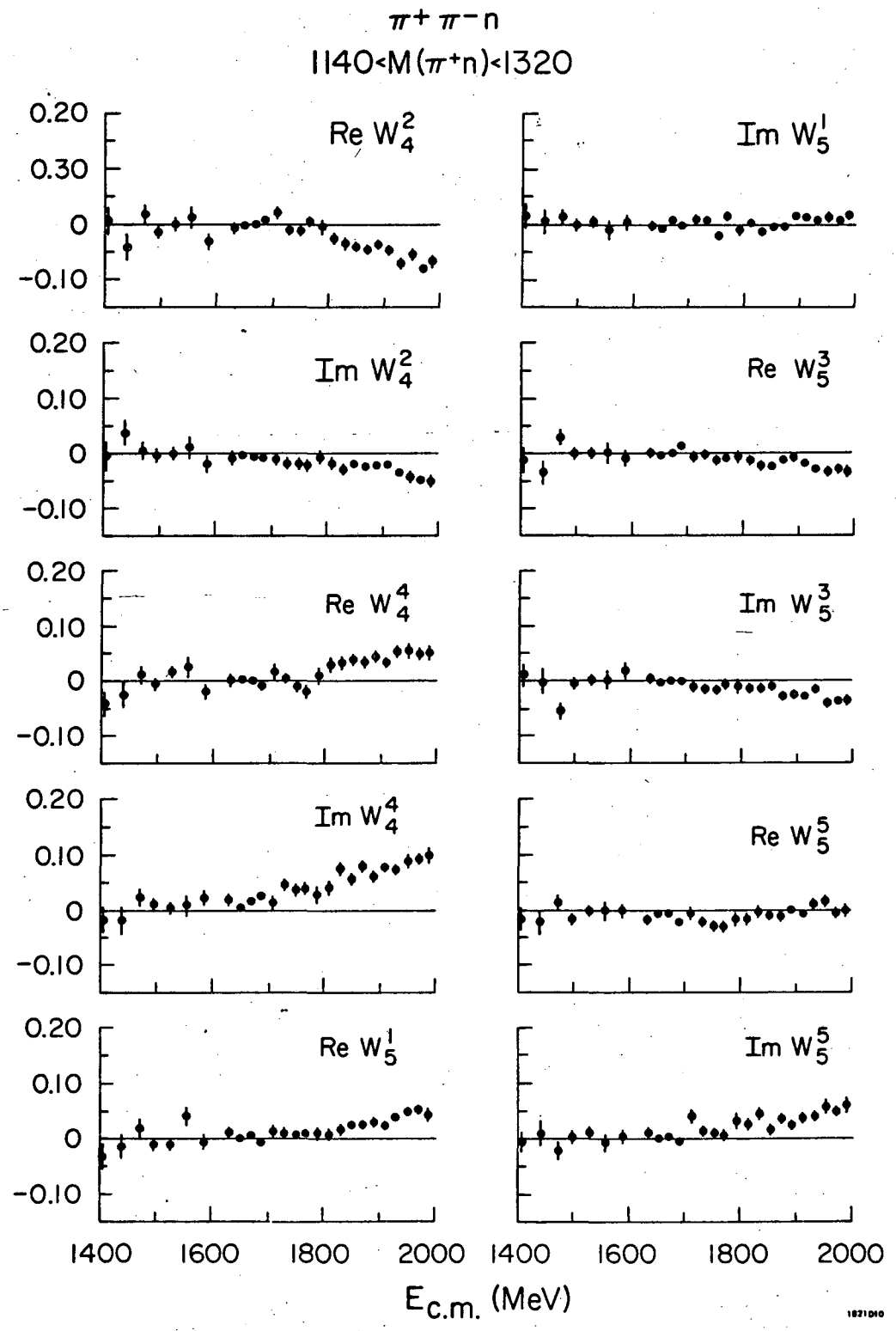
π+ π− n
1140<M(π+n)<1320
Re W$_4^2$
Im W$_5^1$
Im W$_4^2$
Re W$_5^3$
Re W$_4^4$
Im W$_5^3$
Im W$_4^4$
Re W$_5^5$
Re W$_5^1$
Im W$_5^5$
0.20
0.30
0.10
0
−0.10
1400
1600
1800
2000
E$_{c.m.}$ (MeV)

Fig. 23B

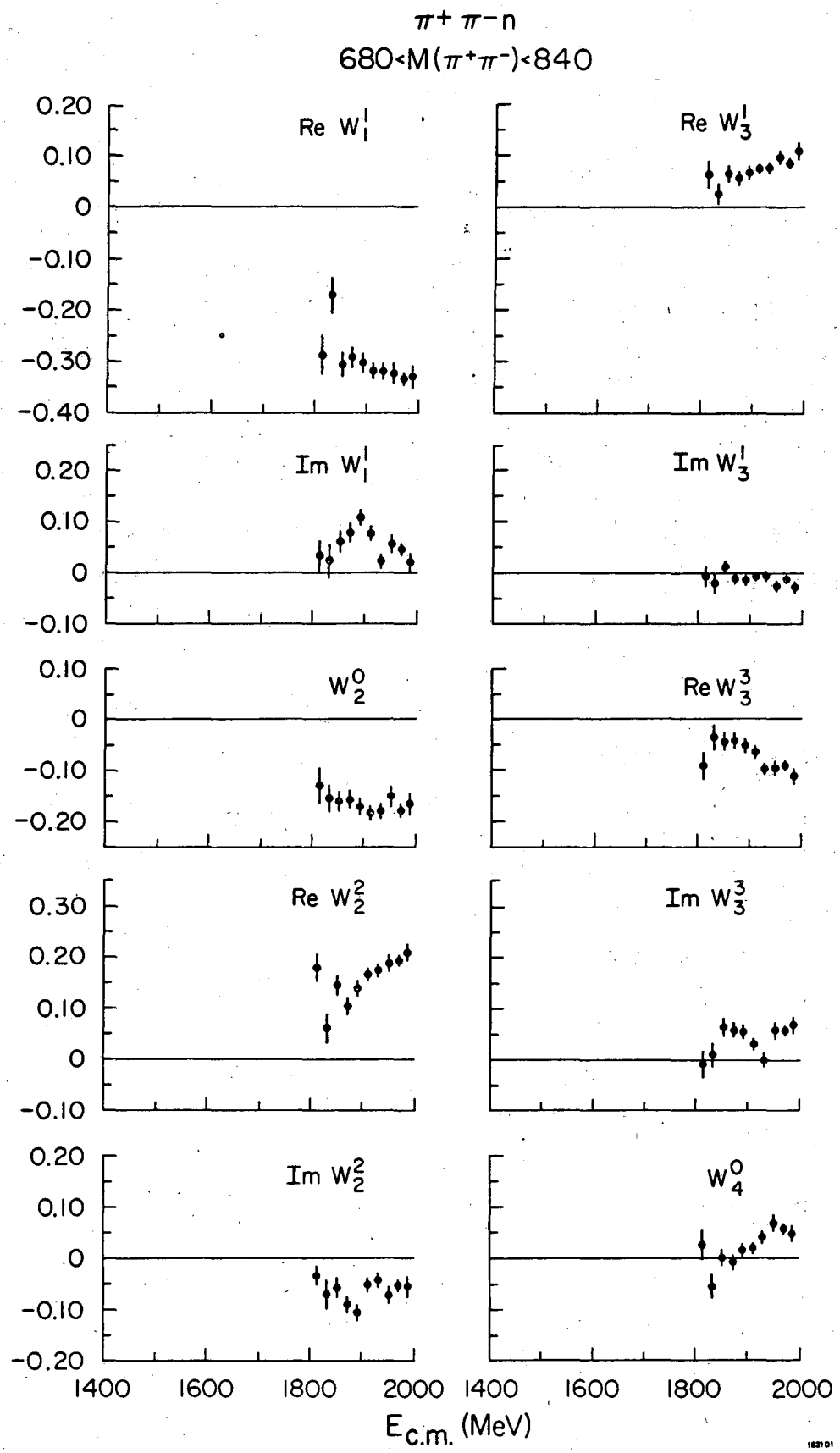
π+ π−n
680<M(π+π−)<840
Re W1I
Re W3I
Im W1I
Im W3I
W2O
Re W3O
Re W2O
Im W3O
Im W2O
W4O
0.20
0.10
0
-0.10
-0.20
-0.30
-0.40
0.30
1400
1600
1800
2000
Ec.m. (MeV)

Fig. 24A

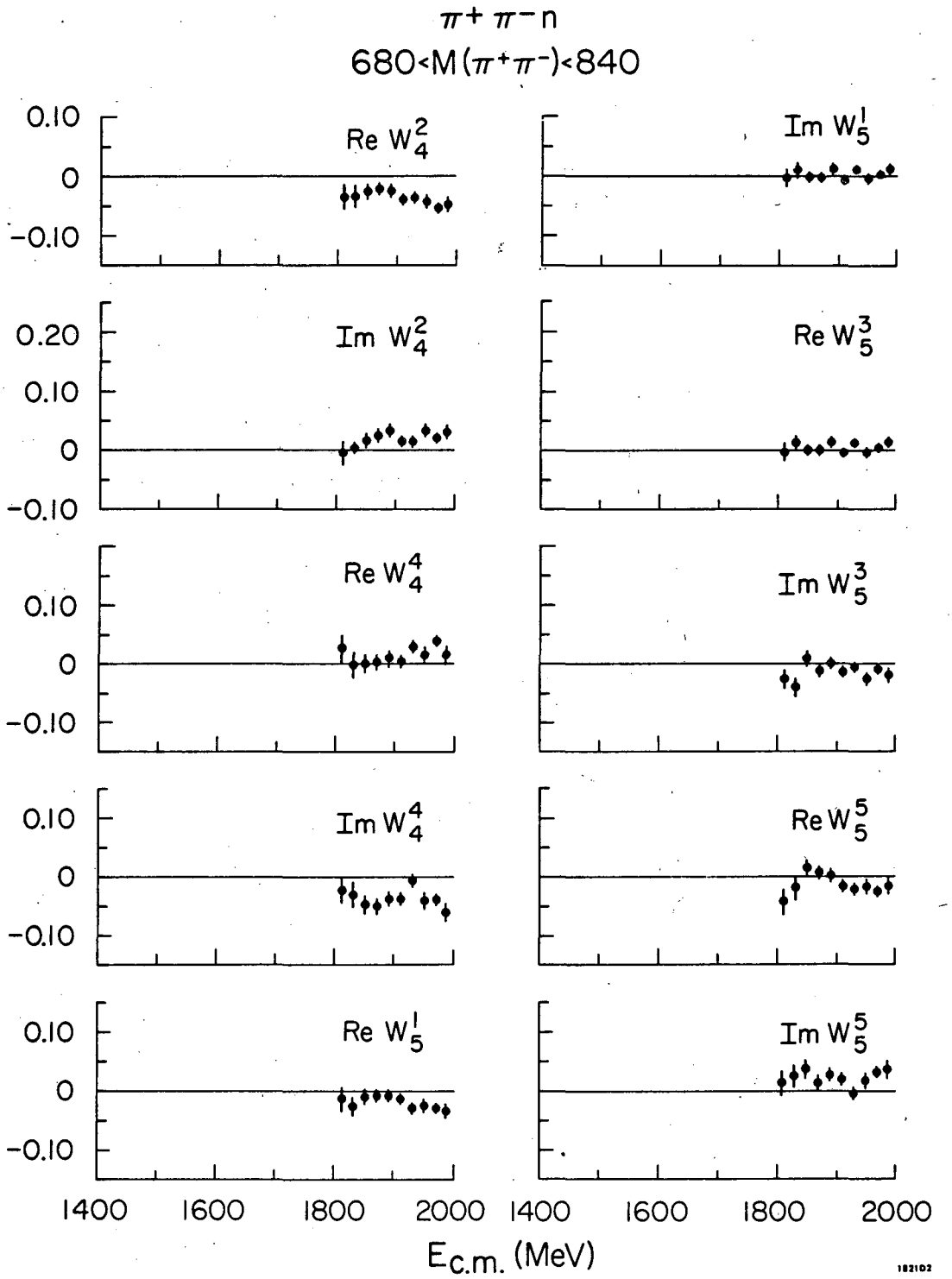
π+ π− n
680<M(π+π−)<840
Re W$_4^2$
Im W$_5^1$
Im W$_4^2$
Re W$_5^3$
Re W$_4^4$
Im W$_5^3$
Im W$_4^4$
Re W$_5^5$
Re W$_5^1$
Im W$_5^5$
0.10
0
−0.10
0.20
1400
1600
1800
2000
E$_{c.m.}$ (MeV)
182102

Fig. 24B

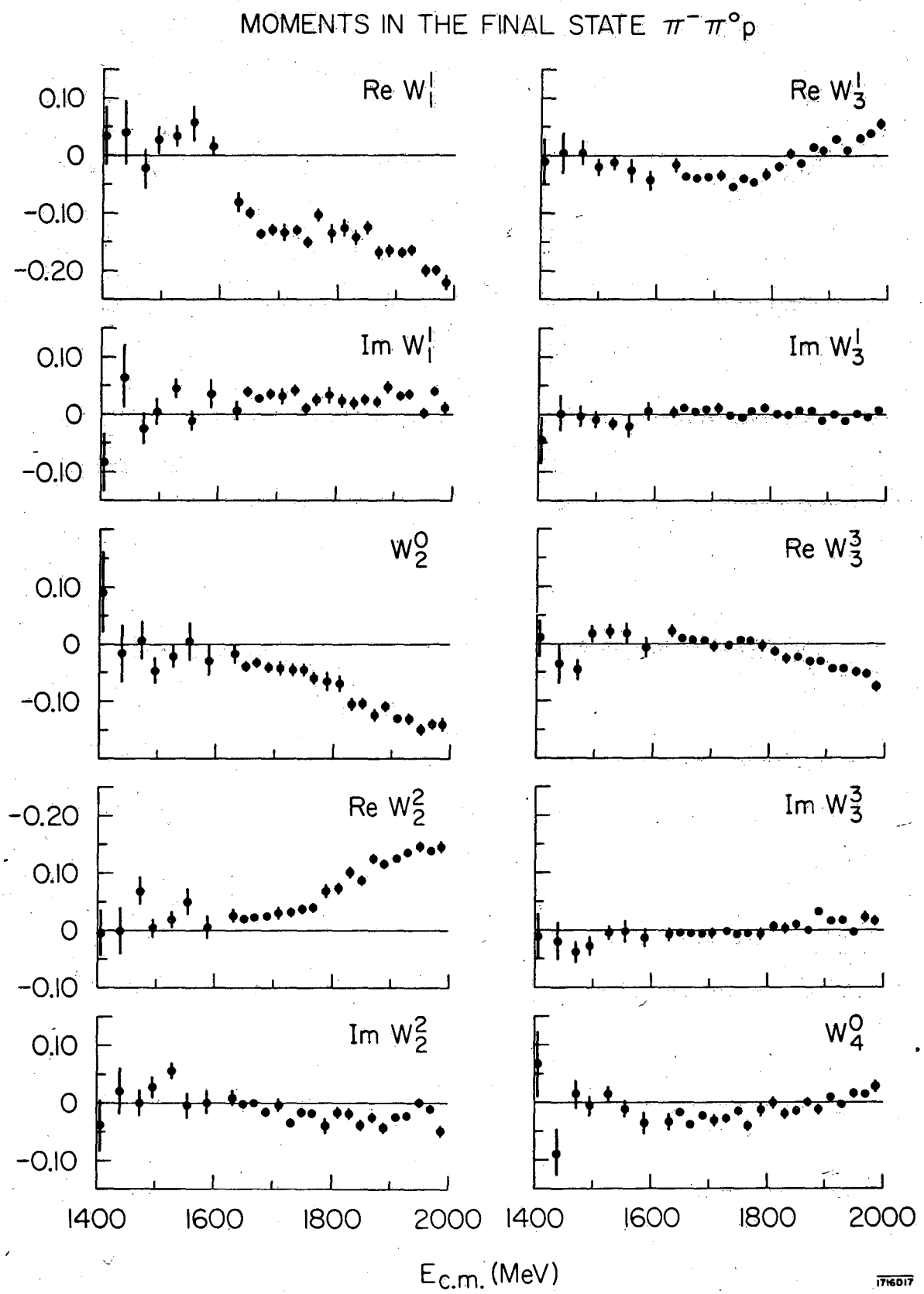
MOMENTS IN THE FINAL STATE $\pi^-\pi^0 p$
Re $W_1^1$
Re $W_3^1$
Im $W_1^1$
Im $W_3^1$
$W_2^0$
Re $W_3^3$
Re $W_2^2$
Im $W_3^3$
Im $W_2^2$
$W_4^0$
0.10
0
-0.10
-0.20
1400
1600
1800
2000
$E_{c.m.}$ (MeV)
1716017

Fig. 25A

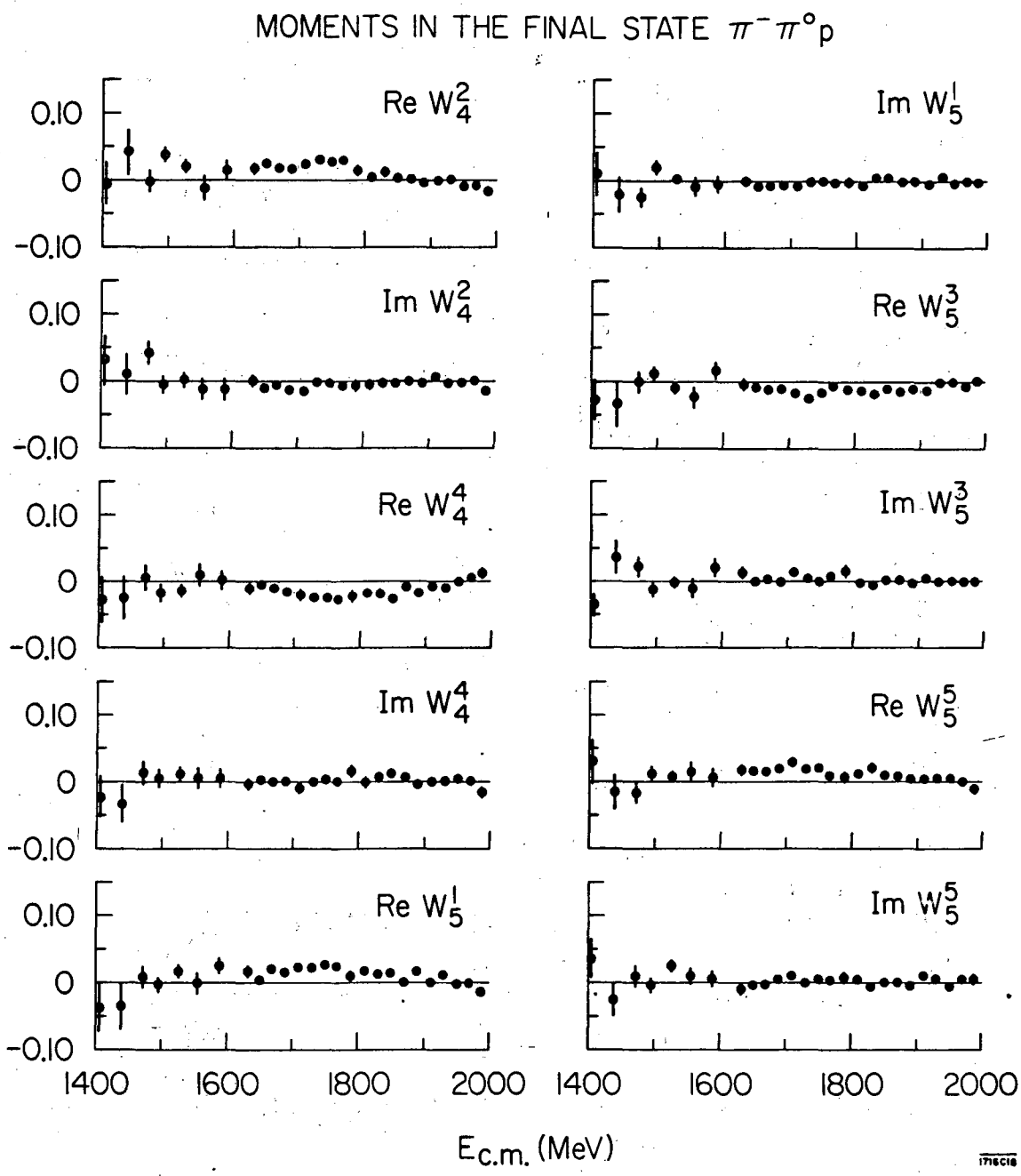
MOMENTS IN THE FINAL STATE $\pi^-\pi^0 p$
Re $W_4^2$
Im $W_5^1$
Im $W_4^2$
Re $W_5^3$
Re $W_4^4$
Im $W_5^3$
Im $W_4^4$
Re $W_5^5$
Re $W_5^1$
Im $W_5^5$
0.10
0
-0.10
1400
1600
1800
2000
$E_{c.m.}$ (MeV)

Fig. 25B

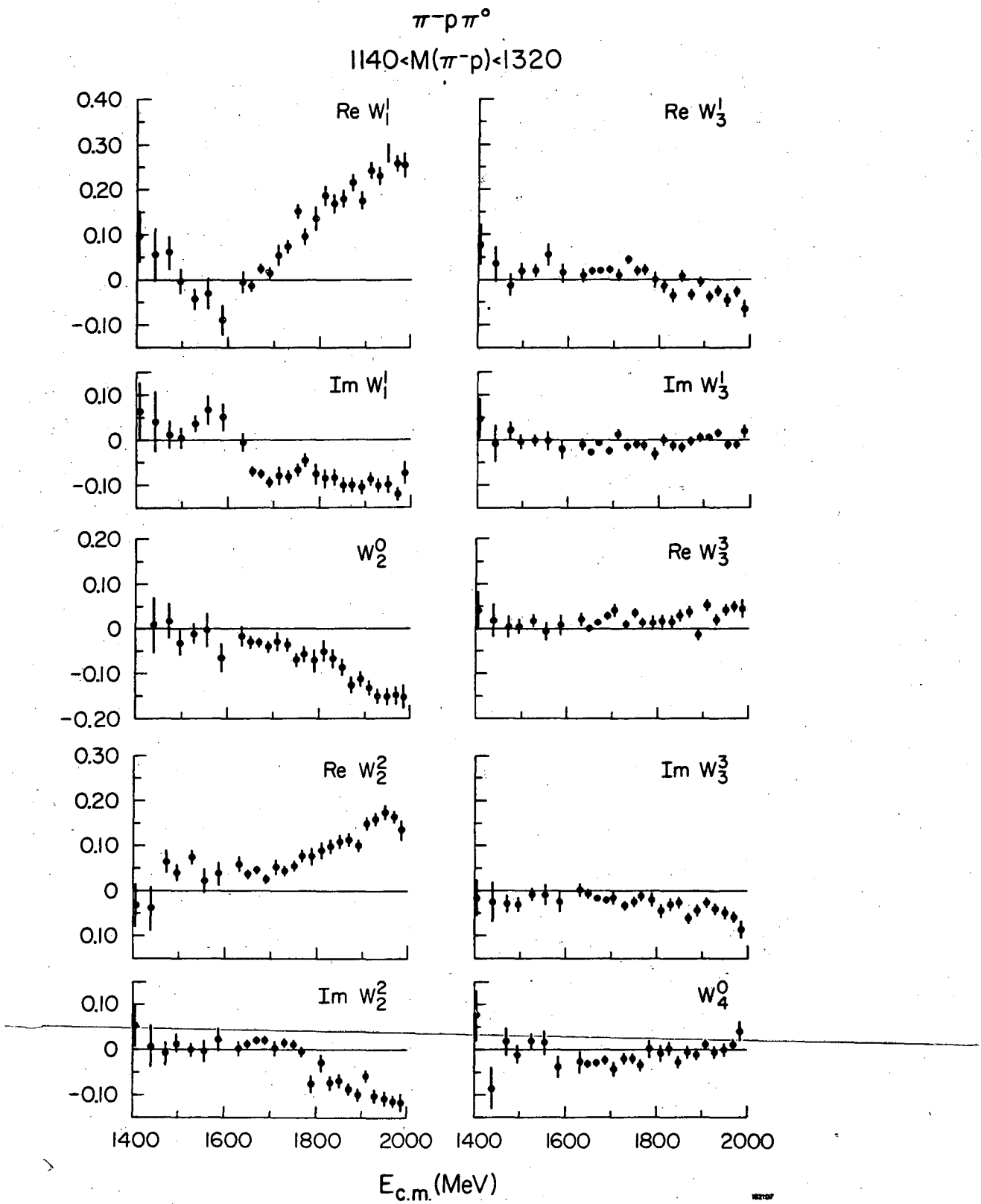
$\pi^- p \pi^0$
$1140 < M(\pi^- p) < 1320$
Re $W_1^1$
Re $W_3^1$
Im $W_1^1$
Im $W_3^1$
$W_2^0$
Re $W_3^3$
Re $W_2^2$
Im $W_3^3$
Im $W_2^2$
$W_4^0$
0.40
0.30
0.20
0.10
0
-0.10
0.20
-0.20
1400
1600
1800
2000
$E_{c.m.}$(MeV)

Fig. 26A

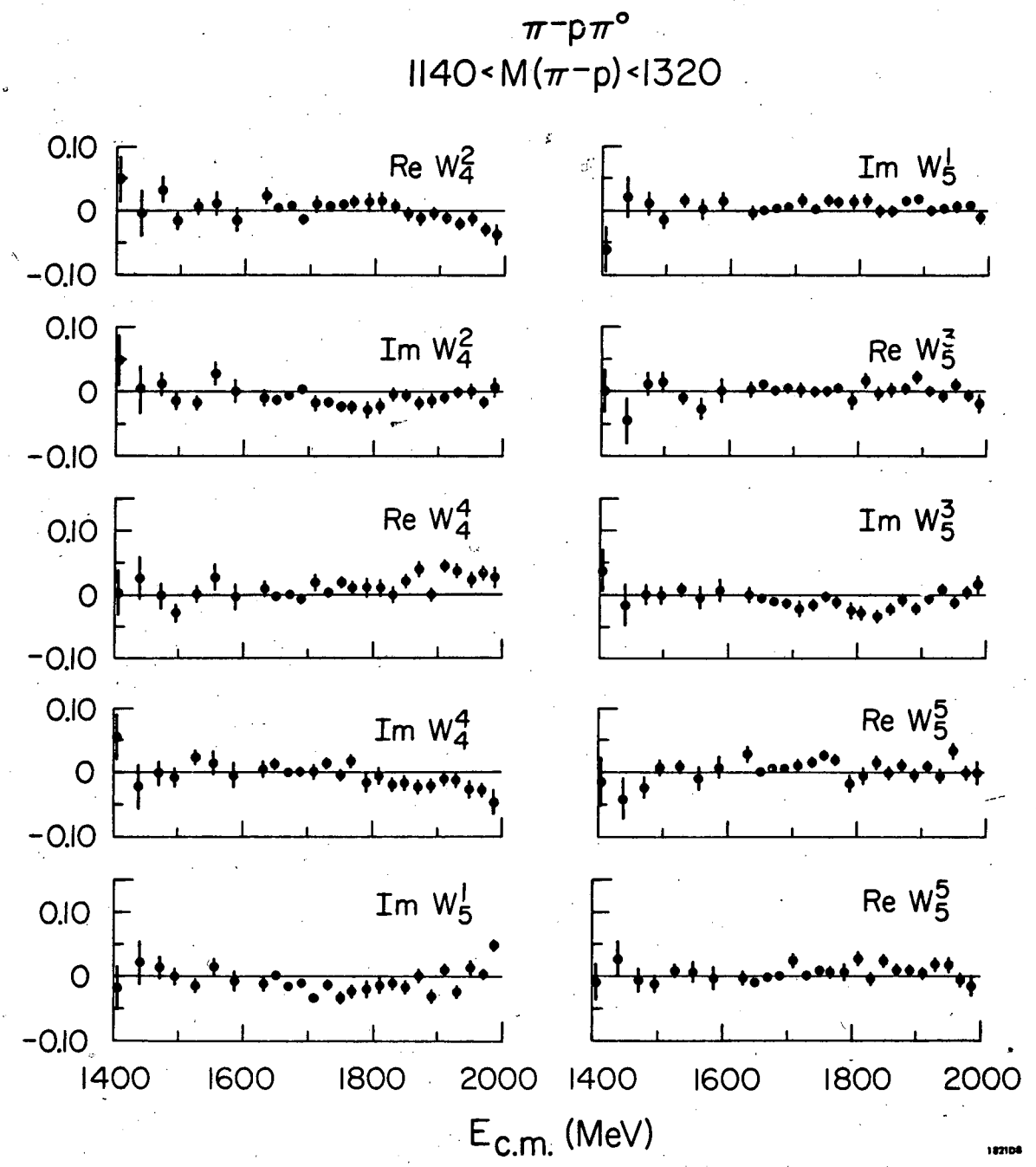
$\pi^- p \pi^0$
$1140 < M(\pi^- p) < 1320$
Re $W_4^2$
Im $W_5^1$
Im $W_4^2$
Re $W_5^3$
Re $W_4^4$
Im $W_5^3$
Im $W_4^4$
Re $W_5^5$
Im $W_5^1$
Re $W_5^5$
0.10
0
-0.10
1400
1600
1800
2000
$E_{c.m.}$ (MeV)

Fig. 26B

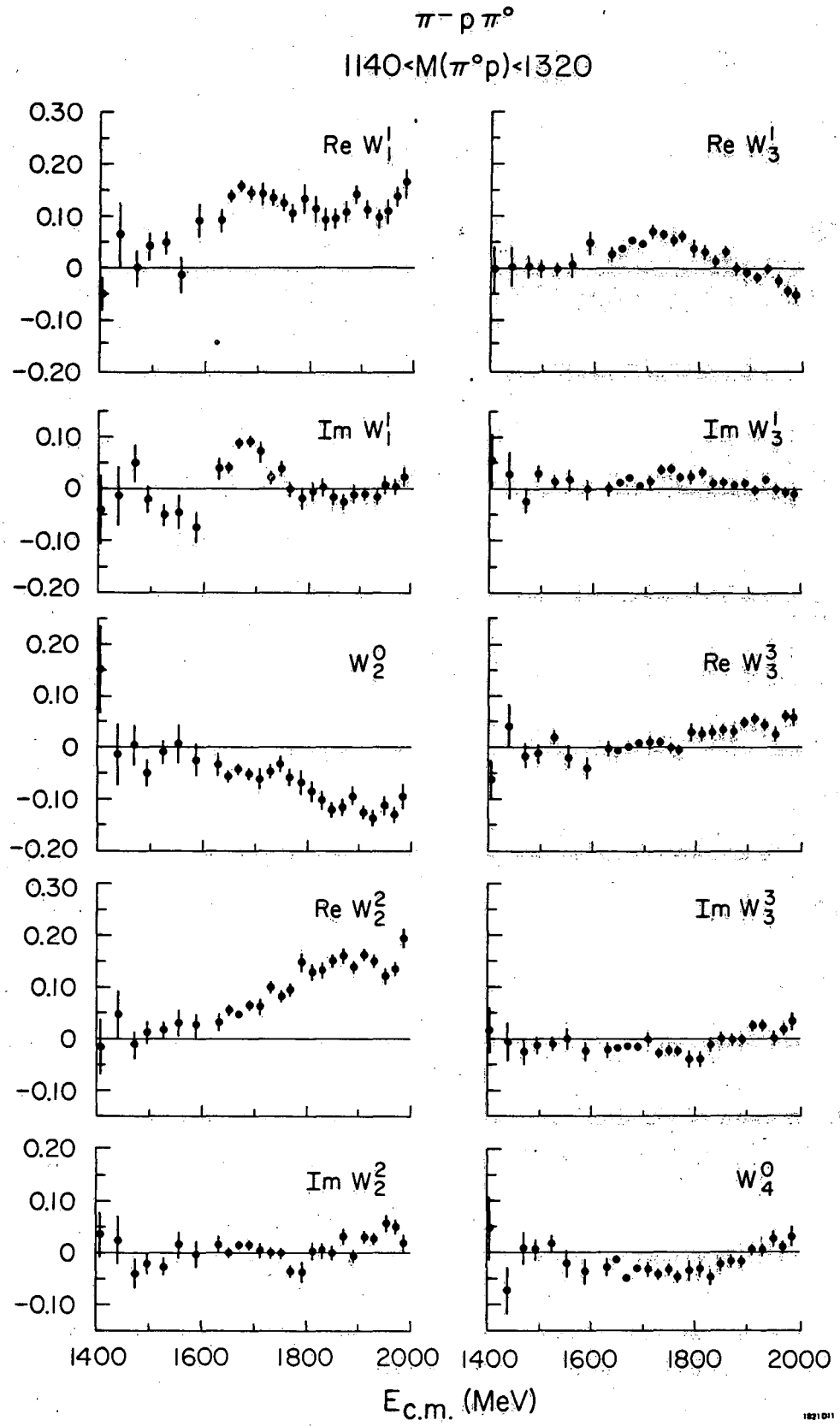
$\pi^- p \pi^0$
$1140 < M(\pi^0 p) < 1320$
Re $W_1^1$
Re $W_3^1$
Im $W_1^1$
Im $W_3^1$
$W_2^0$
Re $W_3^3$
Re $W_2^2$
Im $W_3^3$
Im $W_2^2$
$W_4^0$
0.30
0.20
0.10
0
-0.10
-0.20
1400
1600
1800
2000
$E_{c.m.}$ (MeV)

Fig. 27A

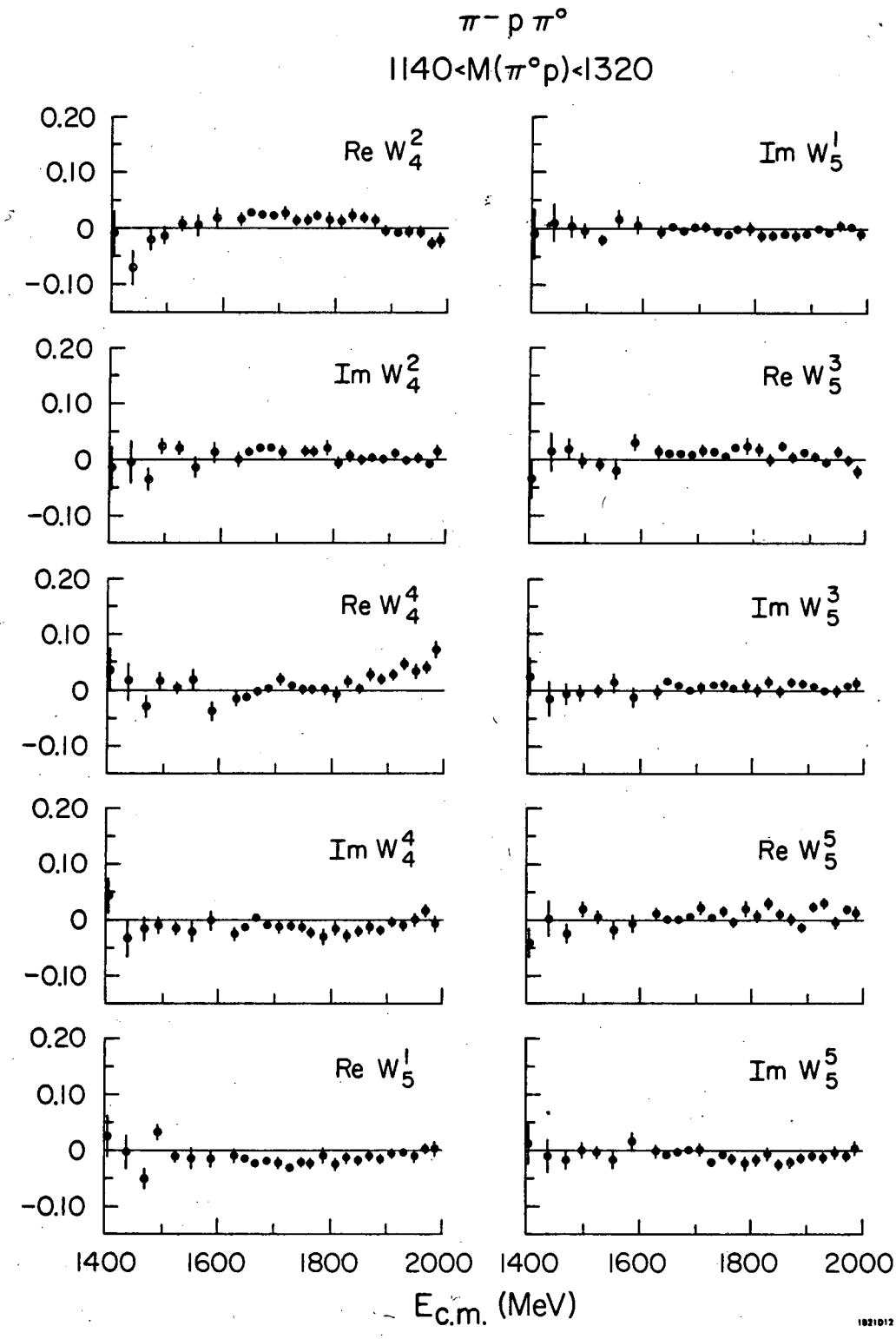
$\pi^- p \pi^0$
$1140 < M(\pi^0 p) < 1320$
Re $W_4^2$
Im $W_5^1$
Im $W_4^2$
Re $W_5^3$
Re $W_4^4$
Im $W_5^3$
Im $W_4^4$
Re $W_5^5$
Re $W_5^1$
Im $W_5^5$
0.20
0.10
0
-0.10
1400
1600
1800
2000
$E_{c.m.}$ (MeV)
1821012

Fig. 27B

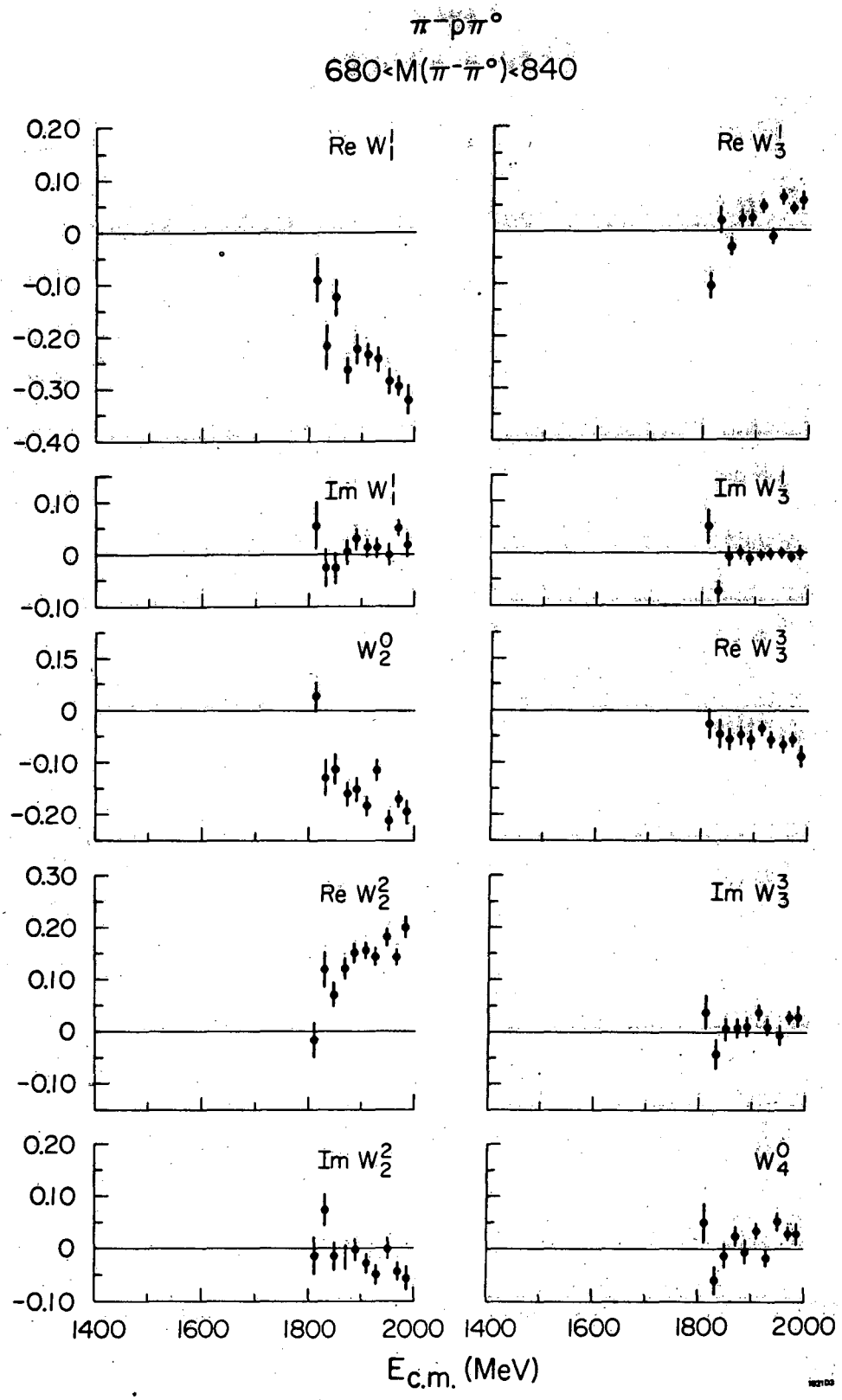
$\pi^- p \pi^0$
$680 < M(\pi^- \pi^0) < 840$
Re $W_1^1$
Re $W_3^1$
Im $W_1^1$
Im $W_3^1$
$W_2^0$
Re $W_3^3$
Re $W_2^2$
Im $W_3^3$
Im $W_2^2$
$W_4^0$
0.20
0.10
0
-0.10
-0.20
-0.30
-0.40
0.15
0.30
1400
1600
1800
2000
$E_{c.m.}$ (MeV)

Fig. 28A

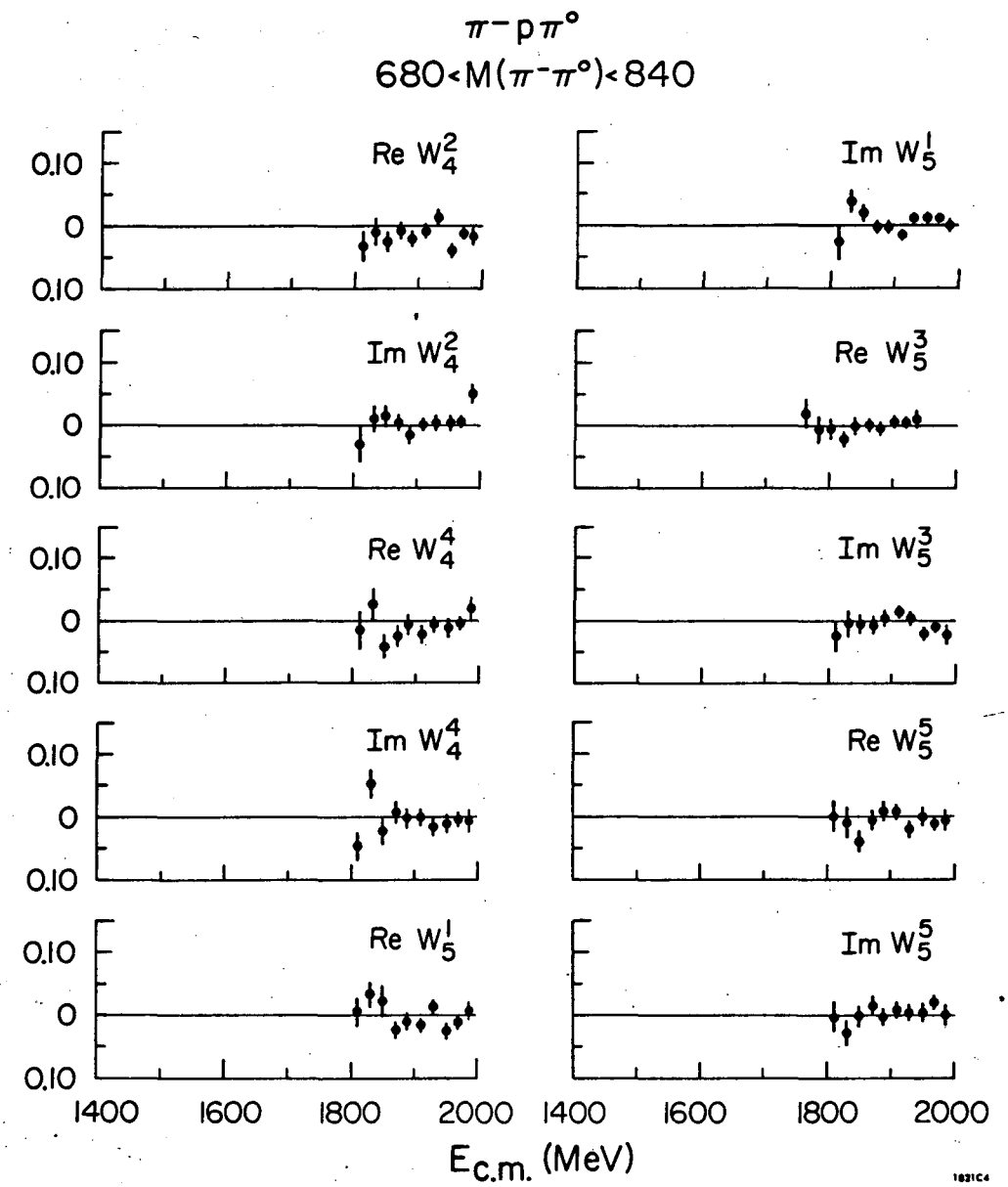
$\pi^- p \pi^0$
$680 < M(\pi^- \pi^0) < 840$
Re $W_4^2$
Im $W_5^1$
Im $W_4^2$
Re $W_5^3$
Re $W_4^4$
Im $W_5^3$
Im $W_4^4$
Re $W_5^5$
Re $W_5^1$
Im $W_5^5$
0.10
0
0.10
1400
1600
1800
2000
$E_{c.m.}$ (MeV)

Fig. 28B

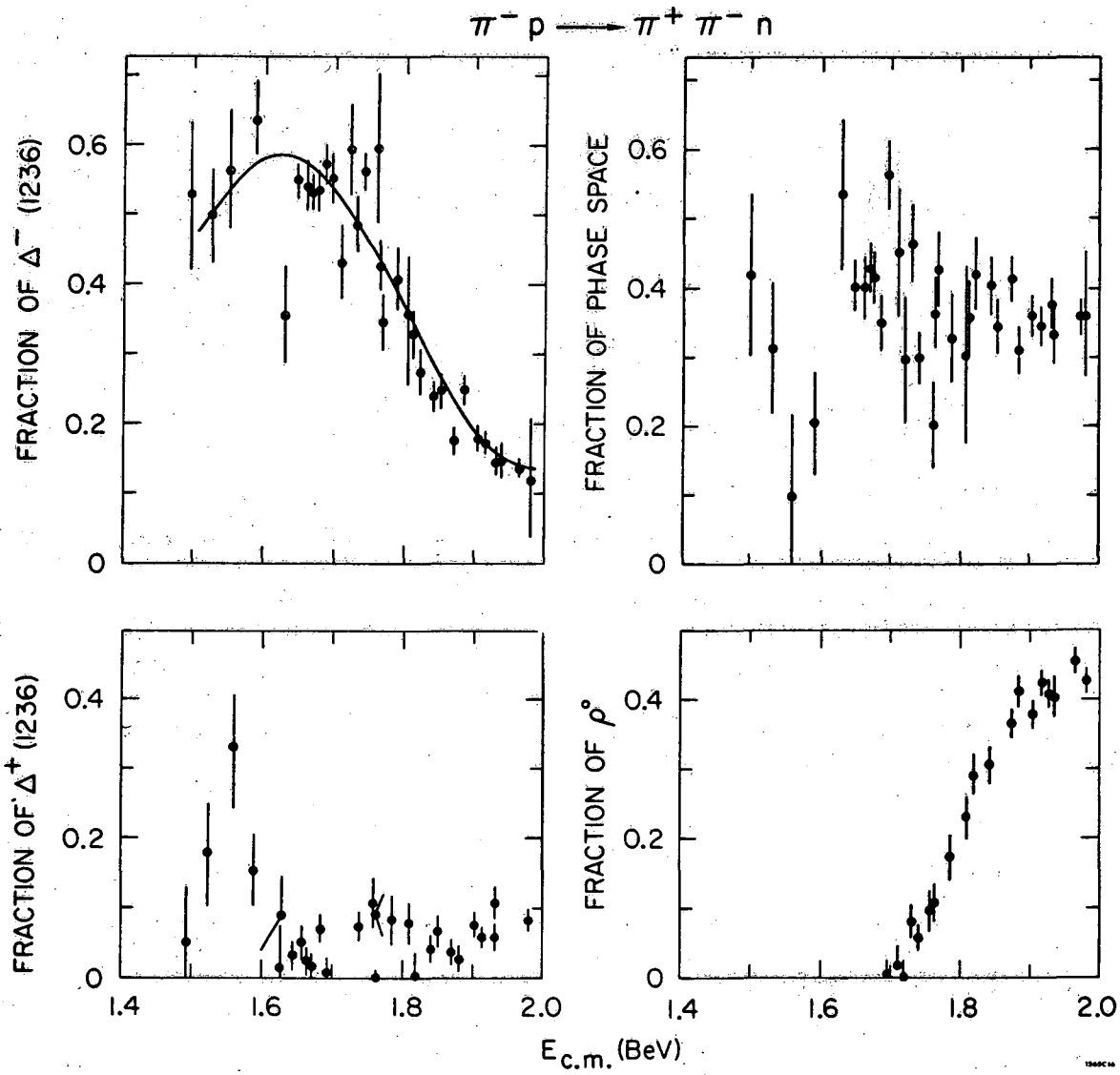
$\pi^- p \longrightarrow \pi^+ \pi^- n$
FRACTION OF $\Delta^-$ (1236)
FRACTION OF PHASE SPACE
FRACTION OF $\Delta^+$ (1236)
FRACTION OF $\rho^0$
0
0.2
0.4
0.6
1.4
1.6
1.8
2.0
$E_{c.m.}$ (BeV)

Fig. 29

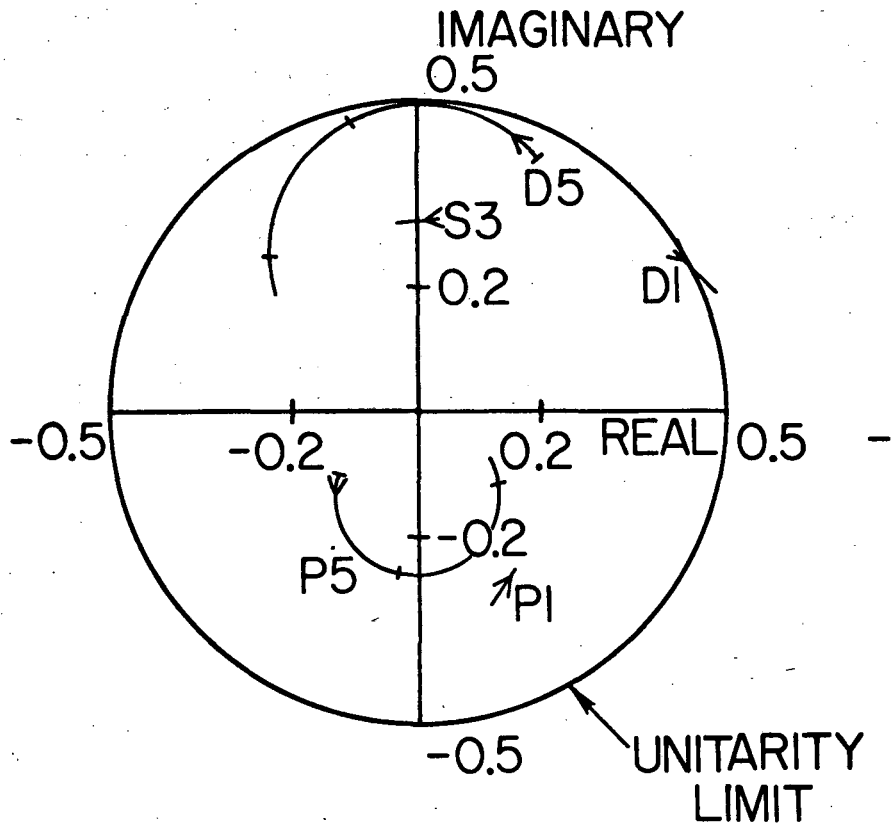


SOLUTION A

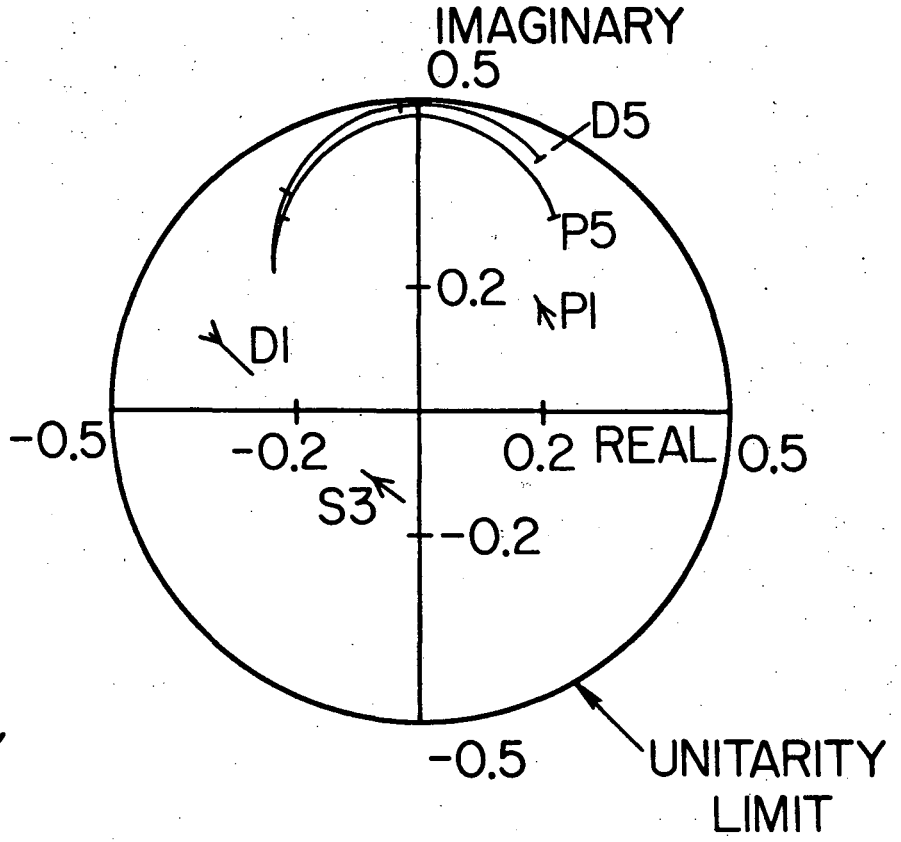


SOLUTION B

177982

Fig 30

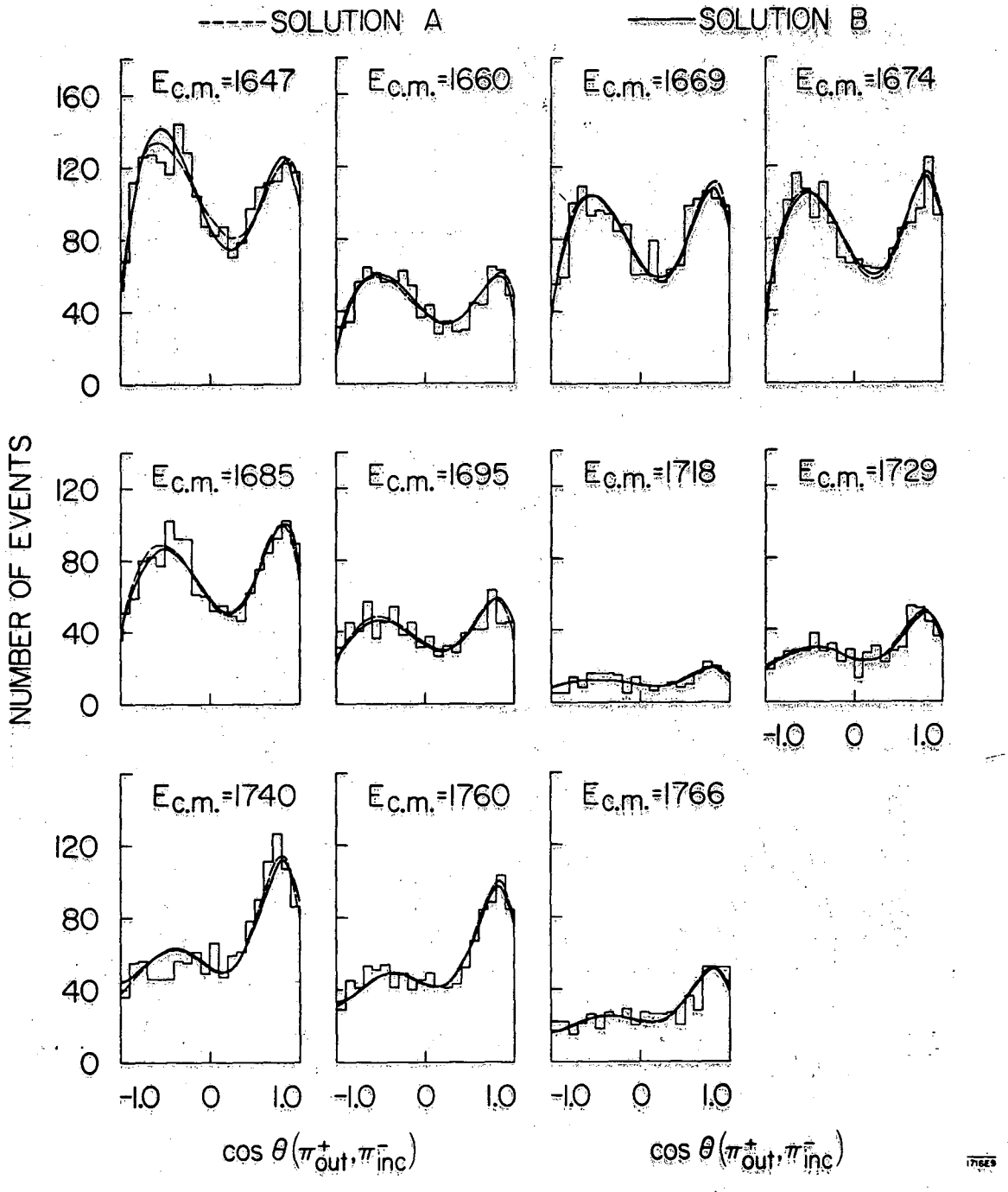
-----SOLUTION A
——SOLUTION B
NUMBER OF EVENTS
Ec.m.=1647
Ec.m.=1660
Ec.m.=1669
Ec.m.=1674
Ec.m.=1685
Ec.m.=1695
Ec.m.=1718
Ec.m.=1729
Ec.m.=1740
Ec.m.=1760
Ec.m.=1766
0
40
80
120
160
-1.0
0
1.0
cos θ(π+out, π−inc)
cos θ(π+out, π−inc)

Fig. 31

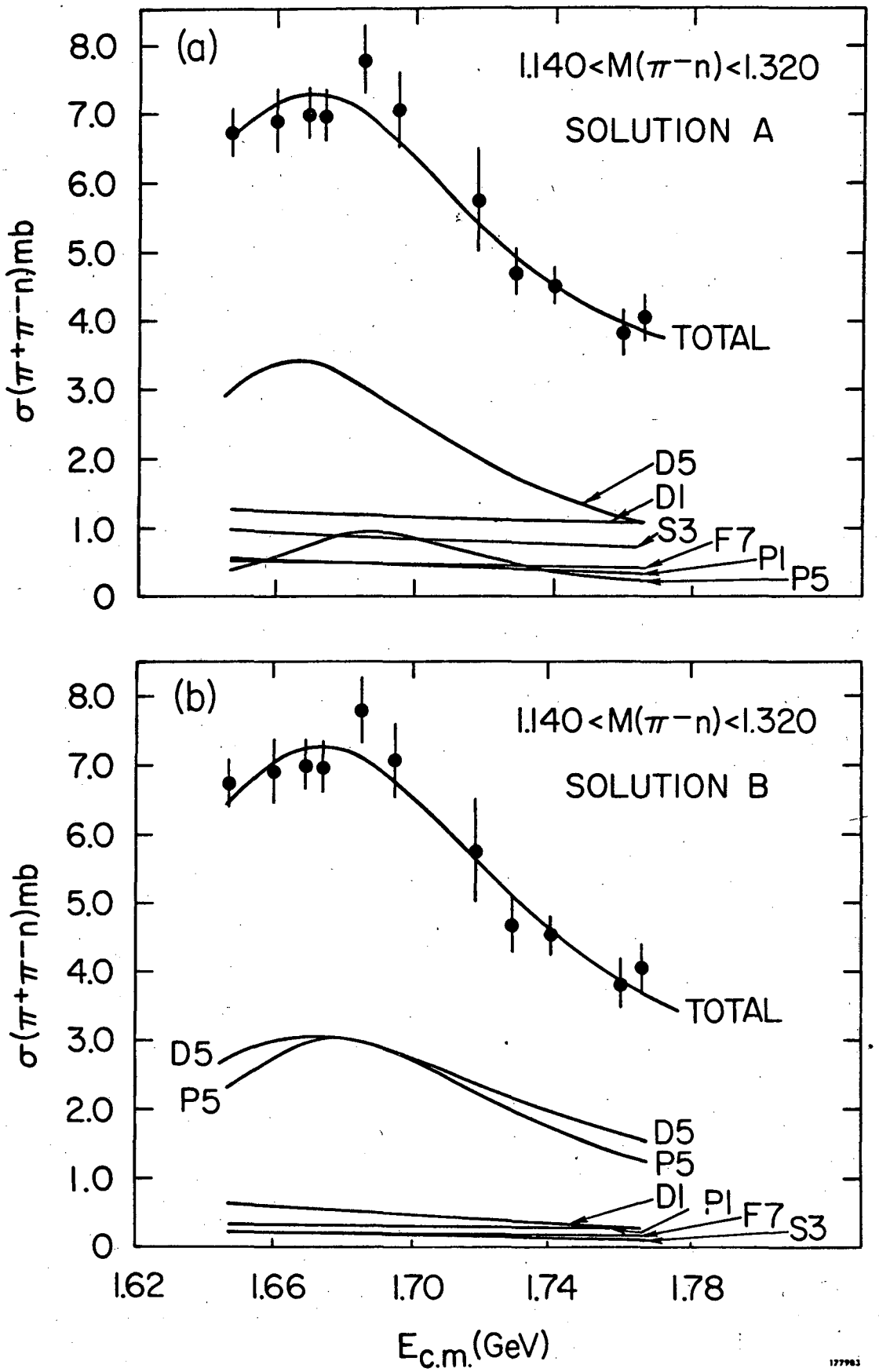
(a)
1.140<M(π⁻n)<1.320
SOLUTION A
TOTAL
D5
DI
S3
F7
PI
P5
(b)
1.140<M(π⁻n)<1.320
SOLUTION B
TOTAL
D5
P5
D5
P5
DI
PI
F7
S3
σ(π⁺π⁻n)mb
8.0
7.0
6.0
5.0
4.0
3.0
2.0
1.0
0
1.62
1.66
1.70
1.74
1.78
E c.m.(GeV)

Fig. 32

LEGAL NOTICE

*This report was prepared as an account of work sponsored by the United States Government. Neither the United States nor the United States Atomic Energy Commission, nor any of their employees, nor any of their contractors, subcontractors, or their employees, makes any warranty, express or implied, or assumes any legal liability or responsibility for the accuracy, completeness or usefulness of any information, apparatus, product or process disclosed, or represents that its use would not infringe privately owned rights.*

*TECHNICAL INFORMATION DIVISION*
*LAWRENCE BERKELEY LABORATORY*
*UNIVERSITY OF CALIFORNIA*
*BERKELEY, CALIFORNIA 94720*